frontiers | Frontiers in Earth Science

TYPE Original Research
PUBLISHED 25 July 2025
DOI 10.3389/feart.2025.1626431

OPEN ACCESS

EDITED BY
Bimlesh Kumar,
Indian Institute of Technology Guwahati, India

REVIEWED BY
Liu Xian,
Northwest University, China
Xin Hu,
Key Laboratory of Biology and Genetic Improvement of Horticultural Crops (North China), China

*CORRESPONDENCE
Jie Xu,
jiexu@cugb.edu.cn

RECEIVED 10 May 2025
ACCEPTED 10 July 2025
PUBLISHED 25 July 2025

CITATION
Qin L, Xu J, Xu D, Liu H and Cai K (2025) Paleogeomorphology reconstruction and its control on sand dispersal systems: a case study from the Pinghu formation in the Hangzhou slope belt, Xihu Sag, East China sea shelf basin.
Front. Earth Sci. 13:1626431.
doi: 10.3389/feart.2025.1626431

Paleogeomorphology reconstruction and its control on sand dispersal systems: a case study from the Pinghu formation in the Hangzhou slope belt, Xihu Sag, East China sea shelf basin

Lanzhi Qin[1], Jie Xu[2,3,4]*, Donghao Xu[1], Hao Liu[2,3,4] and Kun Cai[1]

[1]CNOOC Shanghai Branch, Shanghai, China, [2]School of Ocean Sciences, China University of Geosciences (Beijing), Beijing, China, [3]Key Laboratory of Polar Geology and Marine Mineral Resources, China University of Geosciences (Beijing), Beijing, China, [4]Hainan institute of China University of Geosciences (Beijing), China University of Geosciences (Beijing), Sanya, Hainan, China

Paleogeomorphology, as a key factor influencing depositional environments, plays a critical role in sedimentary processes and sediment distribution. Although considerable re-search has been conducted on paleogeomorphology and its control on sand bodies in the Xihu Sag, most studies have focused on reconstructing the overall geomorphic framework of the basin. However, limited attention has been given to the fine-scale reconstruction of intra-basin micro-geomorphology and its control on the types and distribution patterns of sedimentary sand bodies, especially the Hangzhou Slope area have received limited attention. This study applies the seismic virtual extrapolation method and mudstone sonic analysis to reconstruct the paleogeomorphology of the Pinghu Formation in the Hang-zhou Slope Belt of the Xihu Sag, aiming to elucidate the control of paleogeomorphic features on sedimentary sand body distribution. Based on detailed geological investigation and sedimentary analysis, combined with paleogeomorphic reconstruction techniques, geomorphic units and their spatial assemblages are identified, and the mechanisms by which variations in paleogeomorphic morphology and slope gradient influence sediment dispersal patterns are revealed. The reconstruction delineates the study area into four zones: steep uplifted areas, gently uplifted areas, slope-basin transitional zones, and basin areas. Integrated with sedimentary facies analysis, it is found that the gently uplifted areas are dominated by delta plain deposits, the slope-basin transitional zones dominated by delta front deposits, and the basin areas dominated by tidal sand ridges and shallow marine mudstones. Micro-geomorphic variations significantly affect sedimentary differentiation across zones. Areas with multiple types of slope breaks and moderate gradients tend to develop delta plain, delta front, and tidal sand ridge deposits; areas with fewer slope break types and gentler slopes favor delta plain and delta front deposition, with limited shelf sands in the delta front; while areas with steeper slopes and fewer slope breaks primarily develop delta plain and delta front deposits. This study enhances the understanding of the interaction between paleogeomorphology and sedimentation and provides new insights

and approaches for paleoenvironmental reconstruction and hydrocarbon exploration.

KEYWORDS

xihu sag, hangzhou slope belt, virtual extrapolation method, paleogeomorphology, sedimentary systems

1 Introduction

Paleogeomorphology represents the original surface morphology of a sedimentary basin during a specific geological period and can be categorized into erosional paleogeomorphology, structural paleogeomorphology, and depositional paleogeomorphology. Erosional and structural paleogeomorphologies reflect the remnant landforms formed at the end of erosion and tectonic activity, respectively, and indicate the magnitude of erosion and the intensity of tectonic movements. Depositional paleogeomorphology refers to the geomorphic characteristics immediately prior to the deposition of a particular strati-graphic unit in a sedimentary basin and provides important clues about environmental changes (Song et al., 2002; Li et al., 2009; Li et al., 2017; Lin et al., 2015; Li et al., 2025). Paleogeomorphological features exert a controlling influence on sedimentary facies types and sand body distribution. The reconstruction of paleogeomorphology facilitates the identification of sedimentary facies and the prediction of sand body distribution (Zhao et al., 2001; Hou et al., 2022; Si et al., 2024; Cheng et al., 2020). Numerous studies, both domestic and international, have investigated the control of paleogeomorphology on sedimentation. These studies consistently demonstrate that paleogeomorphology primarily controls sedimentation by influencing sedimentary types and distribution patterns. Specifically, the overall paleogeomorphic background governs the type of depositional systems, while individual geomorphic units exert a more direct control on the distribution of sedimentary sand bodies (Liu et al., 2019; Hou et al., 2018).

As one of the Mesozoic–Cenozoic petroliferous basins with abundant hydrocarbon resources in China's offshore areas, the East China Sea Shelf Basin hosts several favorable hydrocarbon-bearing sub-basins, among which the Xihu Sag is one of the primary exploration targets (Li and Li, 2003). Significant progress has been made in previous studies on the control of paleogeomorphology on sedimentation in the Xihu Sag. Chen et al. (2025) reconstructed the paleogeomorphology of the middle Pinghu Formation by restoring the structural morphology of the target layer to its depositional-time configuration using a balanced section approach. They found that during the deposition of the middle Pinghu Formation, the paleogeomorphology exhibited a northwest-high to southeast-low structural trend. The source area at Haijiao showed steep slopes, while the depositional area had gentler slopes, forming a subtle submarine uplift. Their analysis indicated that both the distribution of depositional systems and sand bodies were jointly controlled by the depositional environment and the paleogeomorphology. Jiang et al. (2022) reconstructed the paleogeomorphology corresponding to key stratigraphic interfaces of the Pinghu Formation in the Baoshi Slope Belt. They analyzed its control on the types and distribution of sedimentary facies, and concluded that the tidal flat depositional system was modulated by geomorphic slope breaks: supratidal facies developed between erosion zones and high-relief slope breaks, intertidal facies between high and low slope breaks, and subtidal facies below the lower slope breaks. Zhang et al. (2022a) conducted a detailed characterization of paleovalley geomorphology in the Pingxi area of the Pinghu Formation using 3D seismic data. They found that in the early stages of deposition, fan-delta deposits con-trolled by paleovalleys were small in scale and spatially restricted. In the later stages, as valleys became infilled and topographic relief decreased, flow velocities declined, and multiple source supply channels contributed to larger, more widespread fan skirts. Yu et al. (2024), based on source area analysis and reconstructed paleogeomorphologic maps of the Baoshi Formation in the Xihu Sag, proposed that the paleogeomorphology during its deposition generally exhibited a northwest-high to southeast-low pattern.

As one of the most favorable hydrocarbon accumulation zones in the Xihu Sag, the western slope belt has demonstrated a high success rate in hydrocarbon drilling and possesses considerable resource potential (Zhang et al., 2022b; Liu et al., 2023a; Wang et al., 2024a). A large number of geological and petroleum exploration studies have been conducted in the western slope belt, yet these efforts have mainly focused on its central and southern parts. In contrast, the Hangzhou Slope Belt has received comparatively limited attention (Wang et al., 2024b; Li et al., 2023a; Zhao, 2022; Hou et al., 2019). To better constrain the spatial and temporal distribution of the depositional systems within the Pinghu Formation and to accelerate hydrocarbon exploration in the Hangzhou Slope Belt of the Xihu Sag, it is imperative to strengthen research on the structural and paleogeomorphic characteristics of the Hangzhou Slope Belt, as well as the development patterns of its sedimentary systems. Particular emphasis should be placed on elucidating the relationship between tectonics, paleogeomorphology, and depositional systems, and their influence on the spatial distribution patterns of sedimentary sand bodies.

2 Regional geological setting

The East China Sea Shelf Basin, located on the eastern margin of the Eurasian Plate, is a Mesozoic–Cenozoic back-arc rift basin that developed on a pre-Sinian crystalline basement. Its formation is closely related to the tectonic activities of the Pacific Plate, the In-do-Australian Plate, and the Philippine Sea Plate (Jiang et al., 2022; Zhang et al., 2020; Qin et al., 2025; Li et al., 2018; Zhao et al., 2016; Dai et al., 2014). The Xihu Sag is situated in the eastern part of the East China Sea Shelf Basin and trends NE-SW. It is one of the largest Mesozoic–Cenozoic petroliferous sags within the basin. To the west, the Xihu Sag is bordered (from north to south) by the Hupijiao Uplift, Changjiang Sag, Haijiao Uplift, Qiantang Sag, and Yushan Low Uplift; to the east, it adjoins the Diaoyudao Anticline

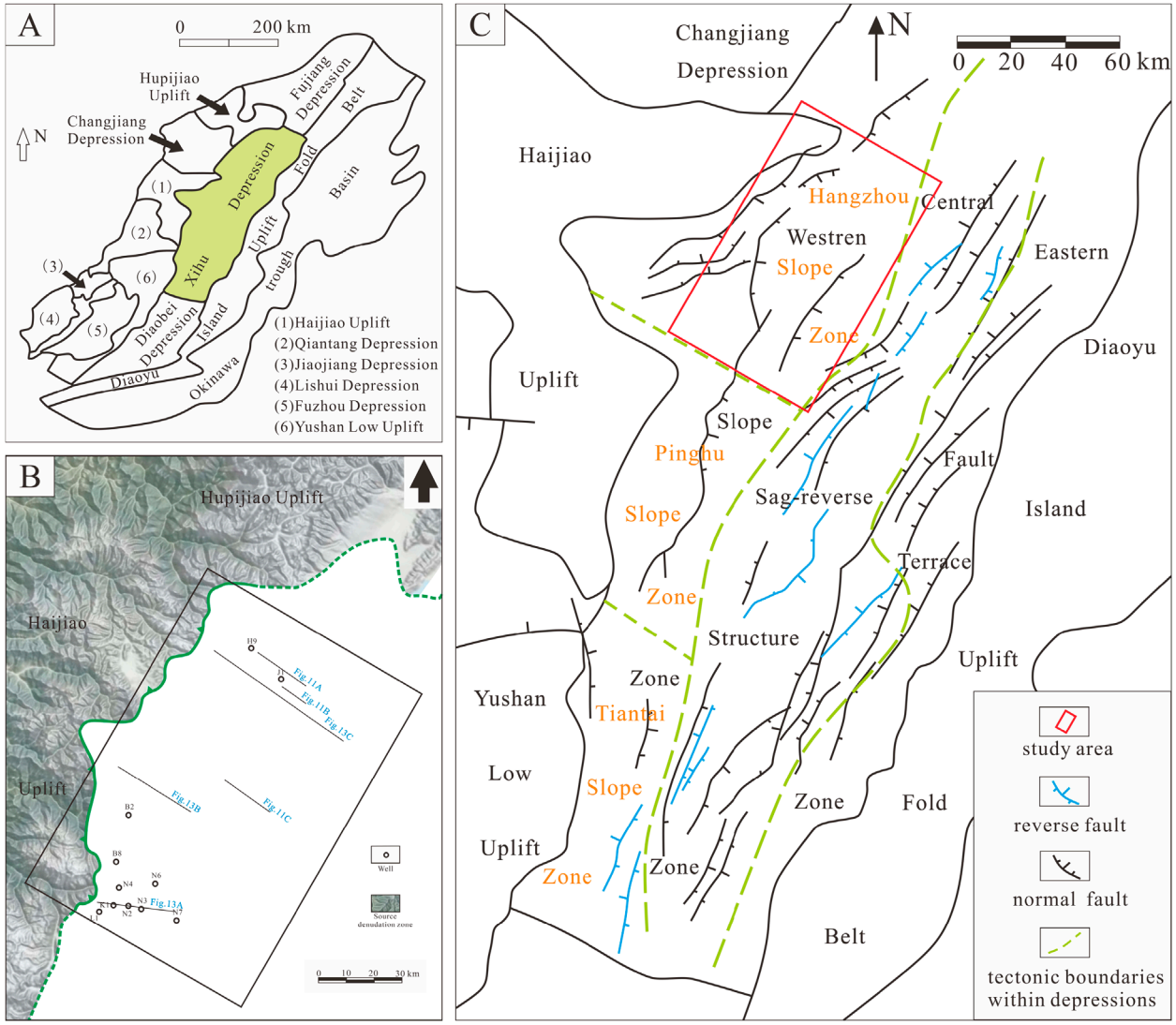

FIGURE 1
Tectonic units of the Xihu Depression. The study area, Hangzhou Slope area is located in the northern part of the western slope. **(A)** The East China Sea Shelf Basin; **(B)** The study area, Hangzhou Slope Zone; **(C)** The Xihu Sag. Modified from Zhang et al. (2014) and Liu et al. (2020).

Belt; to the north, it is adjacent to the Fujiang Sag; and to the south, it borders the Diaobei Sag (Yang et al., 2024; Zhang et al., 2014; Liu et al., 2020) (Figure 1).

The Xihu Sag is approximately 430 km long and 120 km wide, covering a total area of around 51,800 km^2 (Chen et al., 2025; Li et al., 2024; Liu, 2010; Xu et al., 2024). The maxi-mum thickness of the Cenozoic siliceous clastic sediment fill exceeds 20,000 m (Qin et al., 2025). The sag exhibits a structural pattern of "east–west zonation and north–south compartmentalization." From west to east, it is divided into the Western Slope Belt, the Central Depression–Inversion Structural Belt, and the Eastern Marginal Fault Belt (Li et al., 2023b; Wang et al., 2022; Wang et al., 2023; Huang et al., 2019). The Western Slope Belt is further subdivided into the Tiantai Slope Belt, Pinghu Slope Belt, and Hangzhou Slope Belt (Figure 1).

Since its formation and development, the Xihu Sag has undergone seven significant tectonic events, namely, the Jilong, Yandang, Oujiang, Yuquan, Huagang, Longjing, and Okinawa Trough movements. Collectively, these events can be grouped into six major stages of tectonic evolution: the initial rifting stage, intensive rifting stage, rift-depression transition stage, depression stage, inversion stage, and regional subsidence stage. These evolutionary phases have resulted in a complex and multi-phase tectonic history for the region (Wu et al., 2025).

The stratigraphic succession of the Xihu Sag, from the basement upward, consists of the Paleocene, Eocene Bajiaoting Formation, Baoshi Formation, and Pinghu Formation; the Oligocene Huagang Formation; the Miocene Longjing, Yuquan, and Liulang formations; the Pliocene Santan Formation; and the Pleistocene Donghai Group (Huang et al., 2022; Li et al., 2023c; Shen et al., 2021; Xu et al., 2024) (Figure 2). The present study focuses on the northern part of the Western Slope Belt of the Xihu Sag, specifically within the Hang-zhou Slope Belt, with the Pinghu Formation as the target stratigraphic interval.

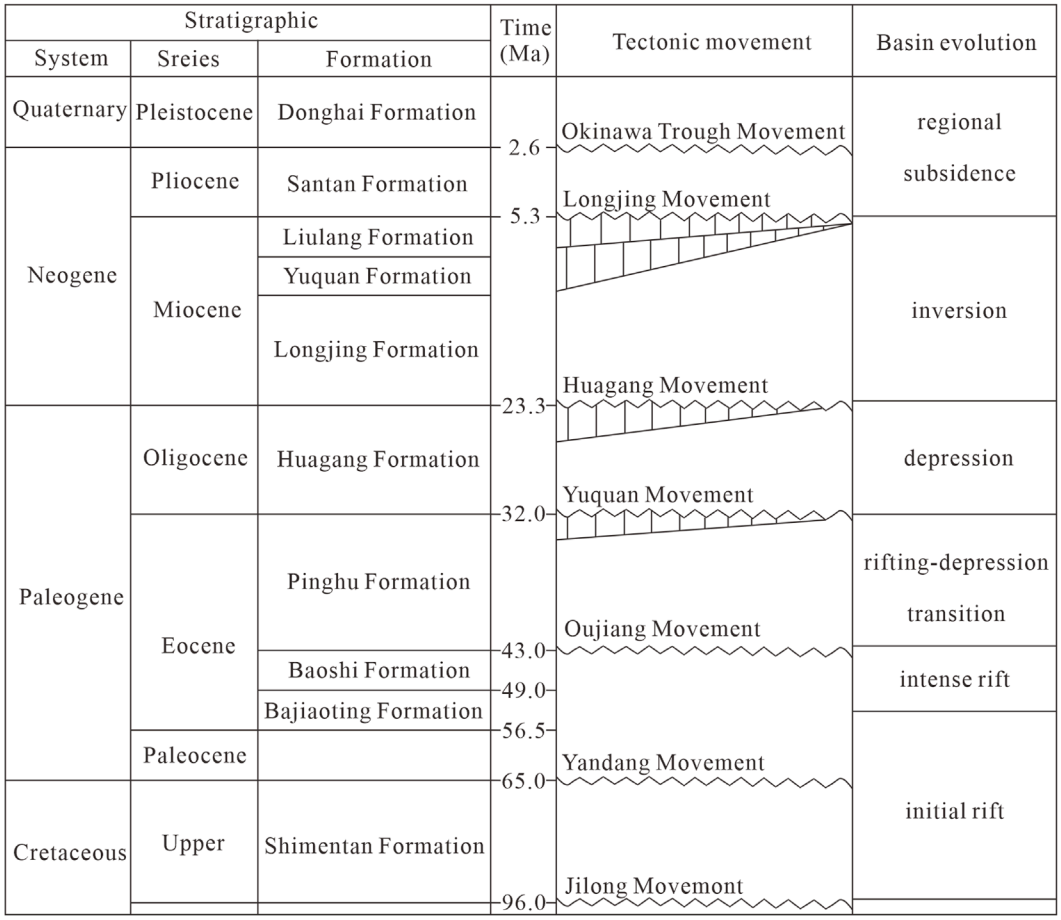

FIGURE 2
Stratigraphic column of the study area. Modified from Lou et al. (2023) and Wang et al. (2024a).

As the primary source and reservoir rock of the Xihu Sag, the Pinghu Formation was deposited between approximately 43 and 32 Ma during the faulting stage of basin evolution. It represents a set of deltaic and tidal flat deposits from the middle to late Eocene and constitutes the core petroleum system in the Xihu Sag. The Pinghu Formation is characterized by thick coal-bearing strata and fine-grained sandstone intervals, with a total thickness ranging from approximately 500–1,500 m. Based on lithological assemblages from base to top, the Pinghu Formation can be divided into three distinct intervals, each with markedly different lithological characteristics.

The lower part of the Pinghu formation contains thick sandstone and thick mudstone layers, along with numerous thin coal seams. In the middle part of the Pinghu formation, thick sandstone bodies are rare or absent, while coal seams are extensively developed and sandstone content is relatively low. The upper part of the Pinghu formation is dominated by thick-bedded medium to coarse sandstones, along with interbedded siltstones and mudstones; coal seams are also present but occur at a much lower frequency (Guo, 2014; Zhao, 2022).

This study focuses on the Pinghu Formation within the Hangzhou Slope Belt. Seismic data are employed to analyze the structural and paleogeomorphic framework and sedimentary systems. The aim is to reconstruct the tectono-paleogeomorphologic features of the study area, identify the types of sedimentary facies developed, and reveal how the structural and paleogeomorphic setting controls the spatial distribution of sedimentary sand bodies. The findings are expected to provide a conceptual model for predicting favorable sandstone development zones in the Hangzhou Slope Belt.

3 Methodology

Restoring the erosion thickness across unconformities and reconstructing paleogeomorphology during key tectonic transformation periods are essential components of hydrocarbon-bearing basin analysis. Numerous researchers, both domestic and international, have proposed a variety of methods for such reconstructions. Commonly used techniques include the virtual extrapolation method, mudstone acoustic transit-time method, sedimentation rate method, stratigraphic correlation, and vitrinite reflectance analysis (Ou, 2014; Liu et al., 2025). Specifically, we now highlight that the virtual extrapolation method is generally based

on a series of idealized assumptions. However, actual geological conditions are often significantly more complex, particularly in areas influenced by faults, folds, and other structural disturbances. In regions with high structural complexity, especially those affected by multiple tectonic events or intense deformation, the virtual extrapolation method may not reliably capture true variations in stratigraphic thickness. Furthermore, the sonic transit time method used to calculate erosion thickness is based on the assumption that mudstone compaction is stable and that there is no significant post-depositional rebound. Although faults are well developed in the study area and the strata have been affected by the later Yuquan movement, the overall structural complexity remains relatively low. Additionally, the mudstone sediments are well compacted, which supports the reasonable applicability of the methods employed in this study. We have clarified these methodological considerations in the revised Introduction and explicitly emphasized the specific innovations and contributions of this study compared to previous paleogeomorphological research in the Xihu Sag. In this study, existing seismic and well logging data are utilized to restore the erosion thickness across key unconformities in the study area using the virtual extrapolation method. For selected local areas, the mudstone acoustic method is applied as a calibration tool. By combining these two approaches, the study aims to accurately reconstruct the eroded thickness of the stratigraphy. This, in turn, facilitates the identification of core paleogeomorphic units—including paleo-uplifts, paleo-valleys, and paleo-slope belts—by determining their development locations, morphological characteristics, and spatial distribution. Furthermore, the study analyzes the developmental features and evolutionary trends of paleogeomorphology in different structural positions.

3.1 Virtual extrapolation method

The virtual extrapolation method (also referred to as the stratigraphic trend extension method) is primarily implemented using seismic interpretation software on interpretation software. It reconstructs the pre-erosional geometric configuration of strata based on seis-mic profiles, thereby allowing for estimation of eroded thickness (Ou, 2014; Xu et al., 2025).

3.1.1 Virtual extrapolation of the basal interface of the target formation

The basal interface of the target formation typically represents the onset of sedimentation for that unit. It may have been affected by tectonic uplift, folding, or other deformation, resulting in erosion. This interface is generally conformable with the overlying strata. Virtual extrapolation of the basal interface involves reconstructing its original extent before erosion occurred. This is achieved by identifying and tracing the seismic reflection characteristics of the overlying strata in areas unaffected by erosion.

When performing virtual extrapolation, it is essential to confirm that the seismic reflections above the interface in the non-eroded zones preserve continuous features, such as onlap, toplap, or parallel to subparallel configurations. Only under such conditions can extrapolation of the interface be considered valid. The restoration should generally follow the stratigraphic order from younger to older units.

3.1.2 Virtual extrapolation of the top interface of the target formation

The top interface of the target formation typically represents the termination of depo-sition. It generally exhibits similar seismic reflection characteristics and spatial distribution as the contemporaneous underlying strata. Virtual extrapolation of the top interface aims to reconstruct the depositional boundary of that geological period before any erosion occurred. In areas unaffected by erosion, the top interface of the target formation corresponds to the basal interface of the overlying formation. Therefore, restoration of the eroded top interface involves identifying the first truncation point observed on seismic profiles and laterally tracing it across the eroded area.

3.1.3 Fault influence

When applying virtual extrapolation for stratigraphic restoration, it is crucial to ac-count for the effects of faulting, especially syndepositional boundary faults, on stratigraphic thickness variations. Differences in thickness between the hanging wall and footwall should be considered. Based on the calculated displacement rates of major syndepositional faults, proportional virtual extrapolation can be performed across boundary faults to ensure structural consistency. A schematic diagram illustrating the seismic-based virtual extrapolation method is shown in Figure 3.

3.2 Mudstone sonic method

This method is based on the relationship between the slope of the sonic transit-time curve of older strata and that of younger strata. Three scenarios are generally considered:

When the slope of the sonic transit-time curve for the older strata is equal to that of the younger strata, and the thickness of overlying sediments above the unconformity is less than the estimated eroded thickness, the transit-time curve of the mudstone beneath the unconformity can be extrapolated upward until it intersects the sonic transit-time logarithmic value at the surface. This intersection point represents the paleo-surface, and the vertical distance between this point and the unconformity is taken as the eroded thickness (Figures 4a–c).

When the slope of the older strata's transit-time curve is greater than that of the younger strata, and the compaction curve of the older strata lies to the left of that of the younger strata, it suggests that the pressure exerted by the younger strata on the older units is less than what was applied by the eroded overburden before erosion occurred. In this case, the sonic transit-time method can be used to estimate the eroded thickness.

However, if the compaction curve of the older strata lies to the right of that of the younger strata, it indicates that the older strata are under compacted below the unconformity. In such cases, the sonic transit-time method is not applicable for reconstructing the eroded thickness (Figures 4d,e).

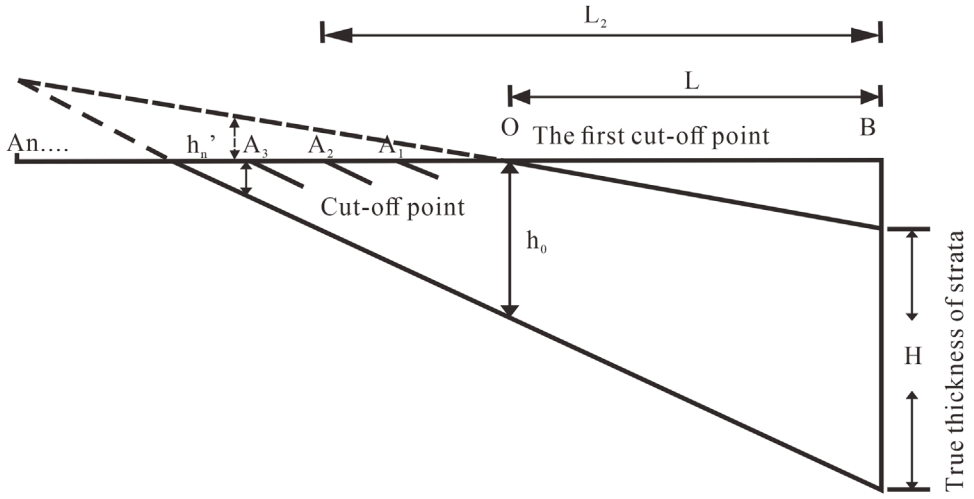

FIGURE 3
Schematic diagram of the virtual extrapolation method.

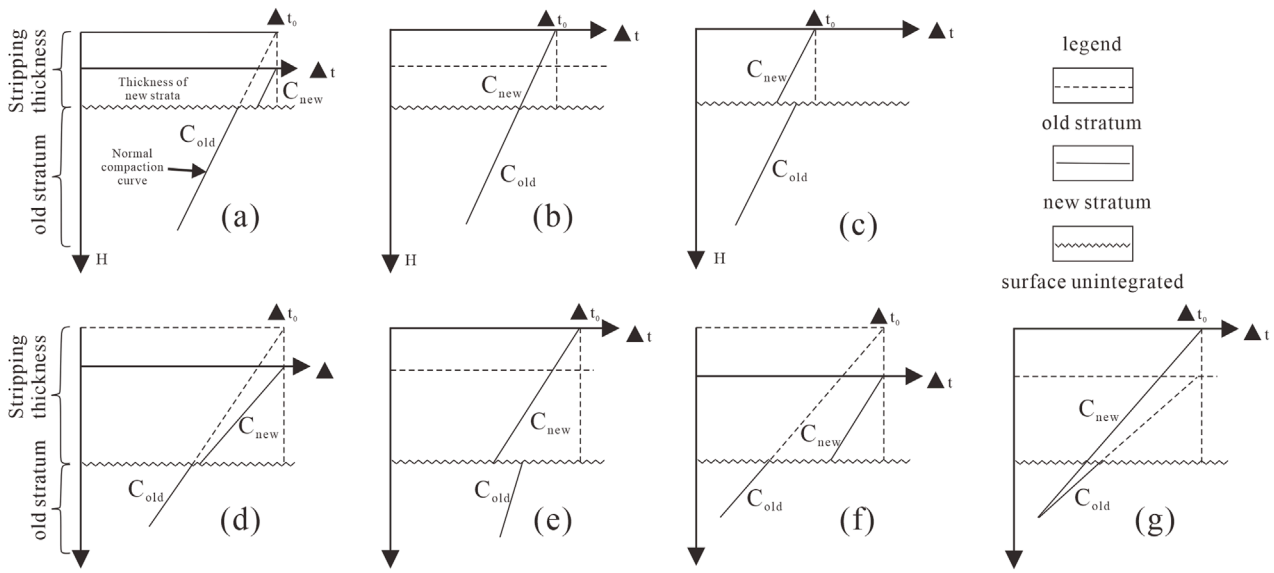

FIGURE 4
Schematic diagram of stratigraphic erosion thickness restoration. **(a)** C_{old} = C_{new}, C_{old} is to the left of C_{new}; **(b)** C_{old} = C_{new}, C_{old} is the same place of C_{new}; **(c)** C_{old} = C_{new}, C_{old} is to the right of C_{new}; **(d)** C_{old} < C_{new}, thickness of new strata < stripping thickness; **(e)** C_{old} < C_{new}, thickness of new strata > stripping thickness; **(f)** C_{old} > C_{new}, C_{old} is to the left of C_{new}; **(g)** C_{old} > C_{new}, C_{old} is to the right of C_{new}. Modified from Ou (2014) and Wei (2014).

When the slope of the sonic transit-time curve for the older strata is less than that of the younger strata, it indicates that the pressure exerted by the younger sediments on the older strata is lower than the pressure once applied by the now-eroded overburden. As a result, the compaction trend of the strata below the unconformity has not been significantly altered. In this scenario, the thickness of the new sediments above the unconformity may be either less than or greater than the eroded thickness. In both cases, the sonic transit-time method remains applicable for reconstructing the eroded thickness (Figures 4f,g) (Mu et al., 2002; Wei, 2014).

4 Tectono-paleogeomorphology reconstruction

4.1 Restoration of stratigraphic erosion thickness

The interpreted seismic horizons within the Pinghu Formation include T40, T34, T33, T32, and T30. Horizon T40 is a second-order sequence boundary and marks the base of the Eocene Pinghu Formation; it is characterized as a regional unconformity.

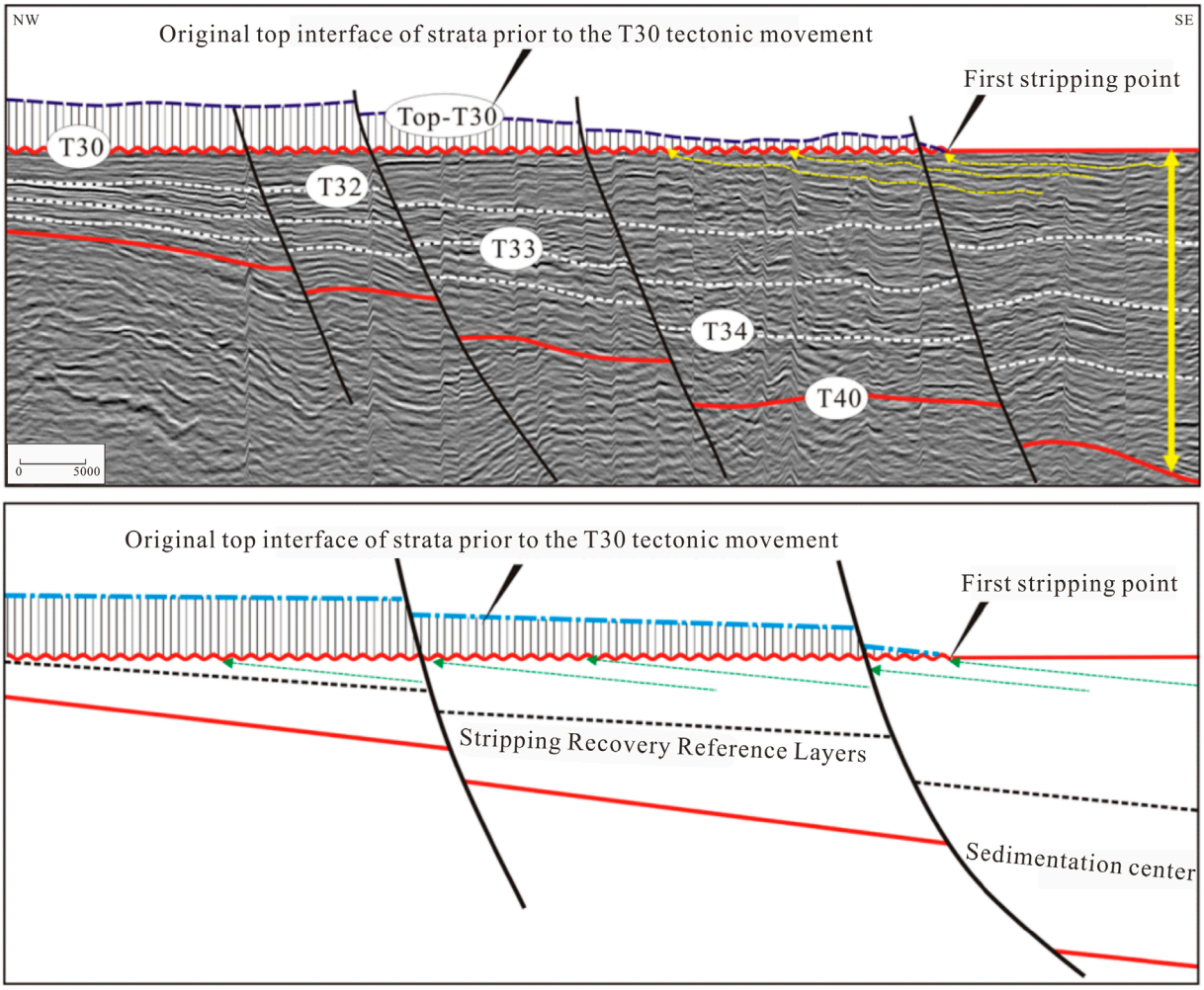

FIGURE 5
Schematic diagram showing seismic virtual extrapolation of the Pinghu Formation in the study area.

T34 is a third-order sequence boundary that separates the lower sub-member of the middle Pinghu Formation from the underlying lower member. T33 is also a third-order sequence boundary, separating the upper and lower sub-members of the middle Pinghu Formation. T32 is a third-order sequence boundary that divides the upper Pinghu Formation from the underlying upper sub-member of the middle Pinghu Formation. T30 is a second-order sequence boundary that marks the base of the Oligocene Huagang Formation and represents an unconformity separating it from the underlying middle to upper Eocene Pinghu Formation, deposited during the syn-rift stage. As the focus of this study is not on establishing a detailed sequence stratigraphic framework, the identification and interpretation of these sequence boundaries are not elaborated further in this section.

Using horizon T30 as an example, the first step is to identify areas where the strati-graphic succession is relatively complete, typically located in the central part of the sag where the strata are thickest. Then, the first truncation point of T30 against the underlying strata is located. Based on the interpreted seismic horizons, T30 is extrapolated in a virtual manner following the trend of the underlying strata (Figure 5).

Four wells within the study area were selected for analysis. For each well, the sonic transit-time curve of the Quaternary strata was used to determine the near-surface sonic transit-time value. An average value was then calculated from the surface sonic transit-times within a defined spatial range, and this average was adopted as the representative surface sonic transit-time value for the area (Table 1).

By inputting the logarithmic surface transit-time value into the derived sonic transit-time regression equations, the paleo-surface depth can be calculated. The erosion thickness for a given formation is then obtained by subtracting the paleo-surface depth from the depth of the corresponding unconformity. Based on this approach, the estimated erosion thicknesses of the Pinghu Formation are as follows: 345 m for Well K1, 288 m for Well L, 317 m for Well N2, and 270 m for Well N3 (Table 1).

Ideally, incorporating a greater number of wells would significantly improve the accuracy of paleogeomorphological reconstruction. However, well coverage in the study area is limited. In the high-uplift regions, due to erosion and poor preservation of the Pinghu Formation strata, no wells have been designed to

TABLE 1 Stratigraphic erosion thickness estimated by the sonic transit-time method for select-ed wells.

Well	Seismic stripping thickness (m)	Surface interval transit time values		Relationship between interval transit time and depth	Old stratigraphic surface (m)	Drilling well stripping thickness (m)
		Empirical formula value	x = lnDT			
K1	310	620	6.43	y = −275.7x+4707.2	2,934	345
L1	255			y = −296.4x+4603	2,697	288
N2	285			y = −274.01x+5,244.5	3,483	317
N3	230			y = −274.16x+5,610.6	3,848	270

penetrate these areas. Similarly, in the deep basin areas, where the Pinghu Formation is buried at depths exceeding 5,000 m, no wells have been drilled to date, as the drilling costs at such depths are prohibitively high in an offshore setting. Consequently, we selected four available wells to conduct the restoration of stratigraphic erosion thickness. This necessarily introduces relatively high uncertainties, particularly in the uplifted and deep basinal regions where well control is absent. Nevertheless, the integration of two independent methods helps to mitigate some of these uncertainties. Despite the data limitations, we believe our study represents a valuable attempt to reconstruct the paleogeomorphology of the area and to enhance the understanding of how paleogeomorphological features have influenced the depositional system.

To improve the objectivity and reliability of erosion thickness restoration, both seis-mic and well log methods were integrated. First, a major integrated well-seismic profile was constructed to perform a comparative analysis between erosion thickness estimates derived from drilling and seismic data (Figure 6). Next, this integrated profile was used as a control line, and erosion thicknesses for different structural units were calculated using their respective methods. Subsequently, region-wide interpretation was conducted based on seismic data to achieve closed structural mapping. Upon completion of the closed interpretation, the erosion thickness resulting from the tectonic activity associated with the T30 horizon was obtained by subtracting the present-day T30 surface from the restored top_T30 interface.

4.2 Paleogeomorphology reconstruction

Paleogeomorphic features exert a fundamental control over sediment source direction, lithology, and formation thickness, thereby directly influencing the types of sedimentary facies and the spatial distribution of sand bodies. Based on the reconstructed tectono-paleogeomorphology of the Pinghu Formation, it is observed that paleogeomorphic highs are mainly located in areas such as the western parts of Hangzhou 35 and Hang Zhou 29, and the western region of the Kongqueting Uplift. The Kongqueting Uplift itself is relatively subdued, forming a weakly developed underwater uplift. The surrounding areas near the major uplifts are characterized as gentle paleohighs with well-developed paleo-valleys, transitioning eastward into broad, gentle slope zones. At this time, the depocenter of the sag was located to the east of the Kongqueting paleohigh.

Overall, the Hangzhou Slope Belt exhibits a paleogeomorphic pattern of north–south segmentation and east–west zoning (Figure 7). From south to north, the region is divided into southern, central, and northern segments. The southern segment features alternating up-lifts and depressions, with a variety of slope break types, including synthetic fault-related slope breaks, reverse fault-related slope breaks, and convergent fault-related slope breaks. The central segment serves as a transitional zone with relatively gentle gradients and is mainly characterized by synthetic fault-related slope breaks. The northern segment has steeper slopes and fewer slope breaks, with relatively simple slope break types.

From west to east, the region can be subdivided into uplift zones, gentle uplift zones, slope zones, and basin zones (Figure 7). Uplift zones are dominated by erosional slope breaks and have provided a stable sediment source over time. Gentle uplift zones contain both fault-related and erosional slope breaks, serving primarily as sediment transport pathways. The slope and basin zones contain multiple slope break types and act as sediment-receiving areas, where various sand dispersal systems are developed (Figure 8). Our paleogeomorphological reconstruction indicates that a significant volume of sediments was later removed by tectonic movements, such as the Yuquan movement (T30), particularly in the high-uplift areas (Figures 5, 8). For example, approximately 230–310 m of strata were eroded by the Yuquan movement, which uplifted the sequence and partially overprinted the original depositional records. This tectonic overprint may lead to misinterpretations, as the proximal sedimentary record has been eroded and is no longer preserved in the present-day data. Our reconstruction helps restore these missing proximal sedimentary records to the current high-uplift areas, suggesting that these regions likely accumulated proximal facies deposits during the depositional period of the Pinghu Formation.

This tectono-paleogeomorphic framework provided the foundational conditions for the spatial distribution of sedimentary facies and sand bodies during the late Pinghu Formation and early Huagang Formation.

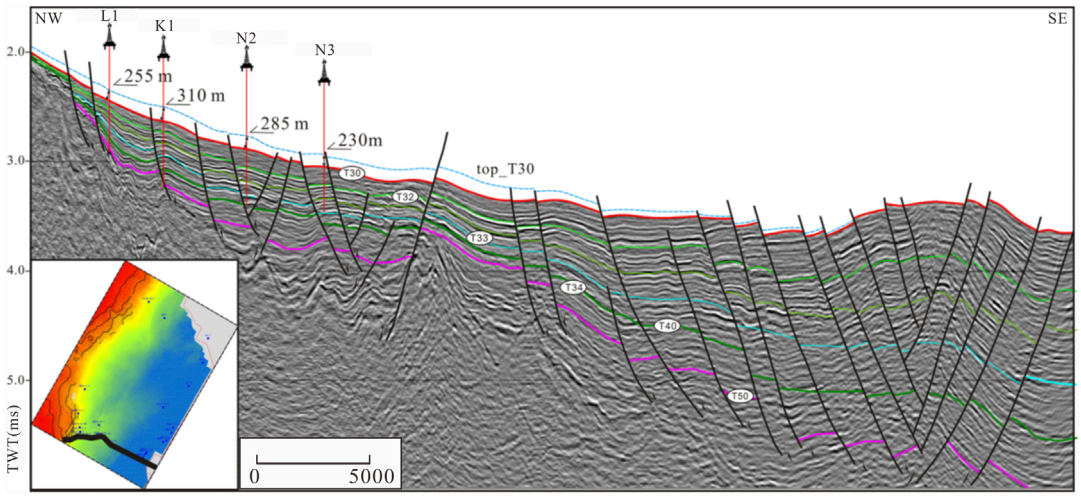

FIGURE 6
Well-seismic integrated erosion thickness restoration for Horizon T30.

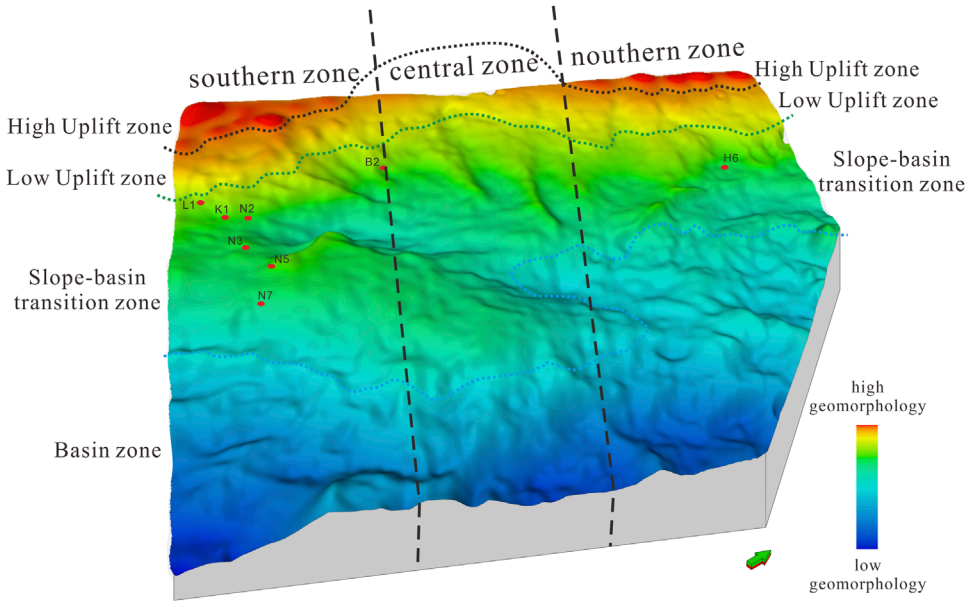

FIGURE 7
Paleogeomorphologic features of the Pinghu Formation basal surface after removal of T30 tectonic influence (Yuquan movement).

Please note the accuracy of the virtual extrapolation method may vary significantly across different structural settings. In relatively stable sag areas, where the strata exhibit gentle dips and consistent thickness trends, the virtual extrapolation method tends to yield reliable results because the assumptions of lateral continuity and uniform deposition generally hold true. In contrast, in slope belt areas, where structural deformation, faulting, and differential subsidence are often more pronounced, the accuracy of the virtual extrapolation method may be reduced. This is because strata in these regions can be laterally truncated, offset, or modified by syn- and post-depositional tectonic activity, introducing greater uncertainty when estimating erosion thickness. We have added this methodological consideration to the revised manuscript to better clarify the method's limitations and its differential applicability across the study area. Despite these uncertainties, our work represents a valuable attempt to improve the understanding of paleogeomorphology in a data-scarce offshore basin, and to provide meaningful insights into how paleogeomorphological features may have influenced the depositional system.

5 Sedimentary system analysis

For additional requirements for specific article types and further information please refer to "Article types" on every Frontiers journal page.

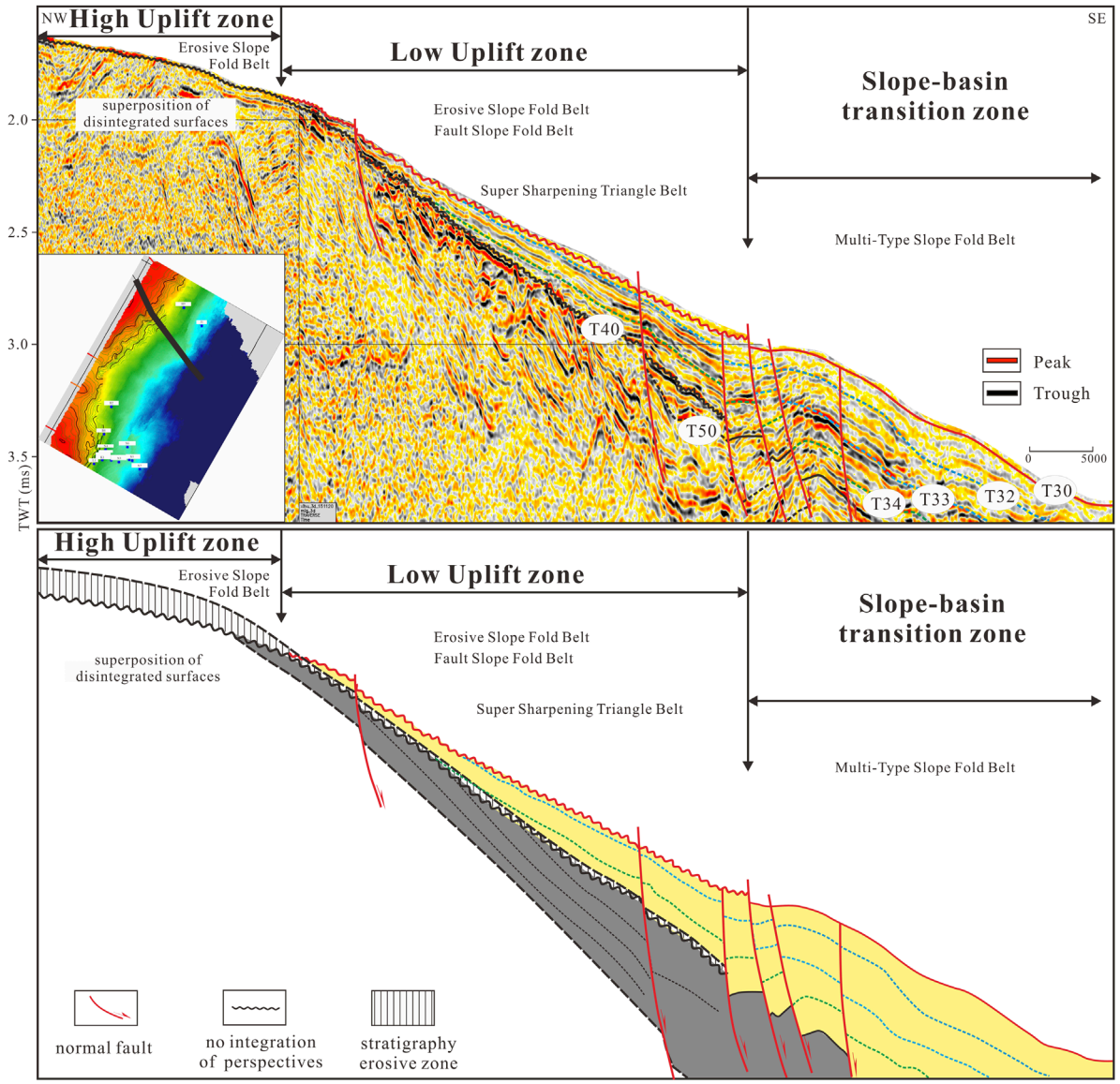

FIGURE 8
Schematic profile of source-to-sink units in the southern part of the study area.

5.1 Current research status of the pinghu formation sedimentary system

Previous studies on the Pinghu Formation are relatively extensive, although they have primarily focused on the Pinghu Slope Belt and its surrounding areas. To date, there are differing interpretations regarding the sedimentary system of the Pinghu Formation. Some scholars have proposed that it represents a tidal flat, tide-dominated delta, and semi-enclosed bay depositional system (Wang et al., 2002; Zhao et al., 2008; Hu et al., 2013; Wei et al., 2013). Others argue that it is mainly composed of fluvial-deltaic deposits and peat swamp systems, with localized influence from marine transgressions (Jiang et al., 2016). There are also viewpoints suggesting that the western slope belt of the sag is dominated by a braided river delta system (Yang et al., 2013). These differing interpretations indicate that the understanding of sedimentary facies within the Pinghu Formation remains somewhat debated. However, for the Hangzhou Slope Belt area, the prevailing view is that a deltaic depositional system is the dominant sedimentary framework (e.g., Yang et al., 2013; Zhao, 2022).

5.2 Core facies

Core observation is a fundamental task in the identification of sedimentary facies and plays a critical role in interpreting depositional environments. Through systematic documentation of lithology, color, grain size, sedimentary structures, and bioturbation features, it is possible to preliminarily determine the depositional settings (Mioumnde et al., 2025). In this study, detailed

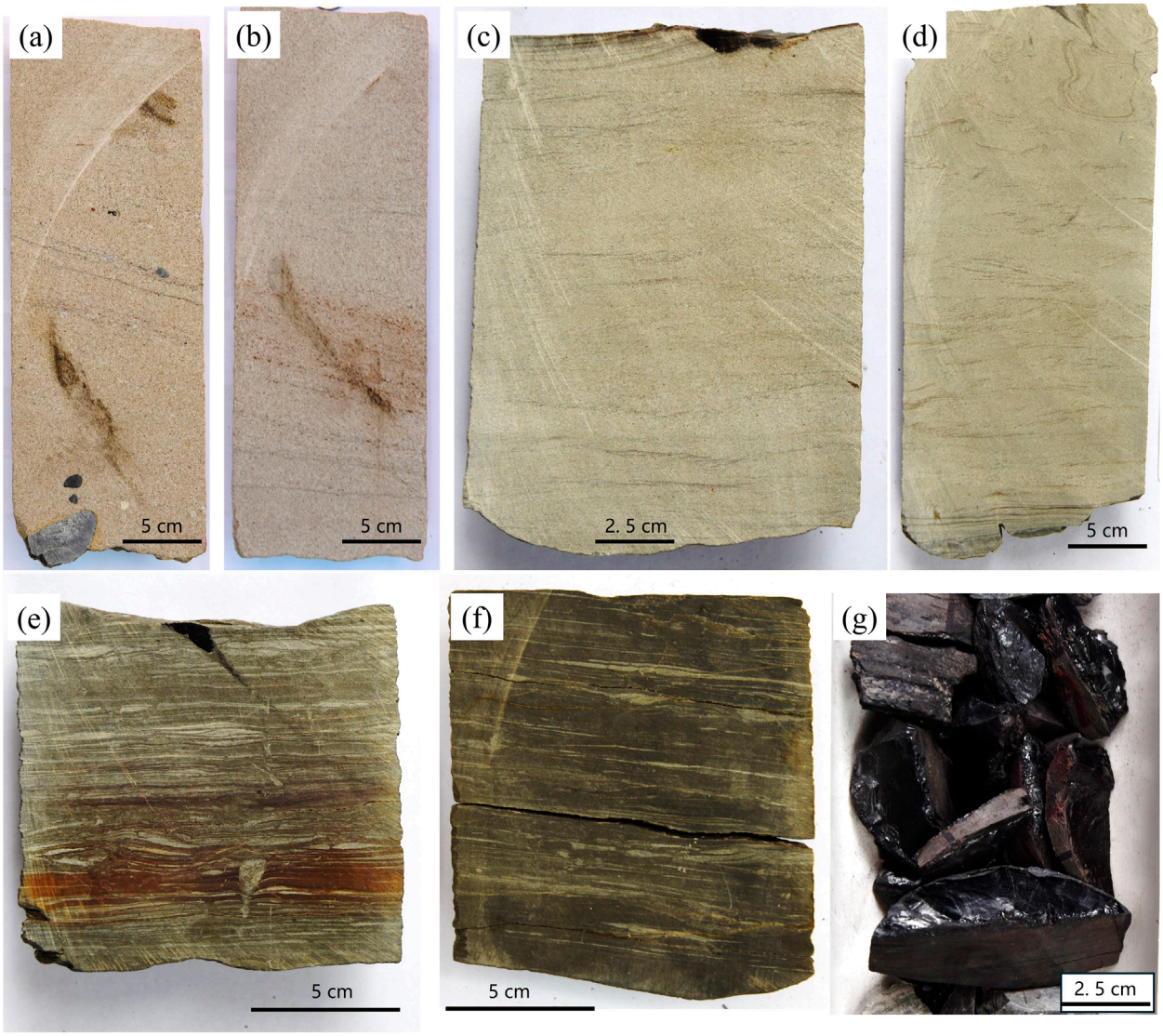

FIGURE 9
Core characteristics of subaqueous distributary channels, subaqueous interdistributary bays, and mouth bars. **(a)** Channel lag deposits of a subaqueous distributary channel showing parallel bedding, Well N2, 4200.47 m; **(b)** Subaqueous distributary channel deposits showing trough cross-bedding, Well N2, 4197 m; **(c)** Wavy bedding of mouth bar, Well N3, 4348 m; **(d)** Wavy bedding of mouth bar, Well N3, 4347 m; **(e)** Subaqueous interdistributary bay deposits showing lenticular bedding, Well N6, 4470 m; **(f)** Subaqueous interdistributary bay deposits showing lenticular bedding, Well N6, 4469 m; **(g)** Subaqueous interdistributary bay deposits containing a coal seam, Well N3, 4352 m.

core observations revealed three major sedimentary facies types in the study area: subaqueous distributary channels, mouth bars, and interdistributary bays.

The subaqueous distributary channels developed at the delta front exhibit typical core characteristics. Prominent scour surfaces and abundant channel-lag gravels are commonly observed at the base. Trough cross bedding is well developed in the middle parts of the channel fill, while parallel bedding is commonly present near the top. Grain size gradually fines upward, displaying a classic fining-upward sequence indicative of decreasing flow energy (Figures 9a, b).

Mouth bars represent another major sand body type within the delta front deposits. Lithologically, they are typically composed of relatively pure, medium-to thin-bedded medium-grained to fine-grained sandstones. These deposits commonly feature wavy cross bedding and coarsening-upward sequences (Figures 9c, d), reflecting sedimentation from decelerating river flows that lose energy upon entering standing water, leading to rapid deposition and mouth bar progradation. In well logs, mouth bars typically present as funnel-shaped or bell-shaped profiles, consistent with their coarsening-upward stacking patterns.

The interdistributary bay facies are mainly composed of gray mudstone and silty mudstone, often interbedded with lenticular sandstones. Core observations reveal features such as low-angle wavy bedding, intense bioturbation, and abundant plant debris (Figures 9 e, f), indicating a relatively low-energy and quiescent

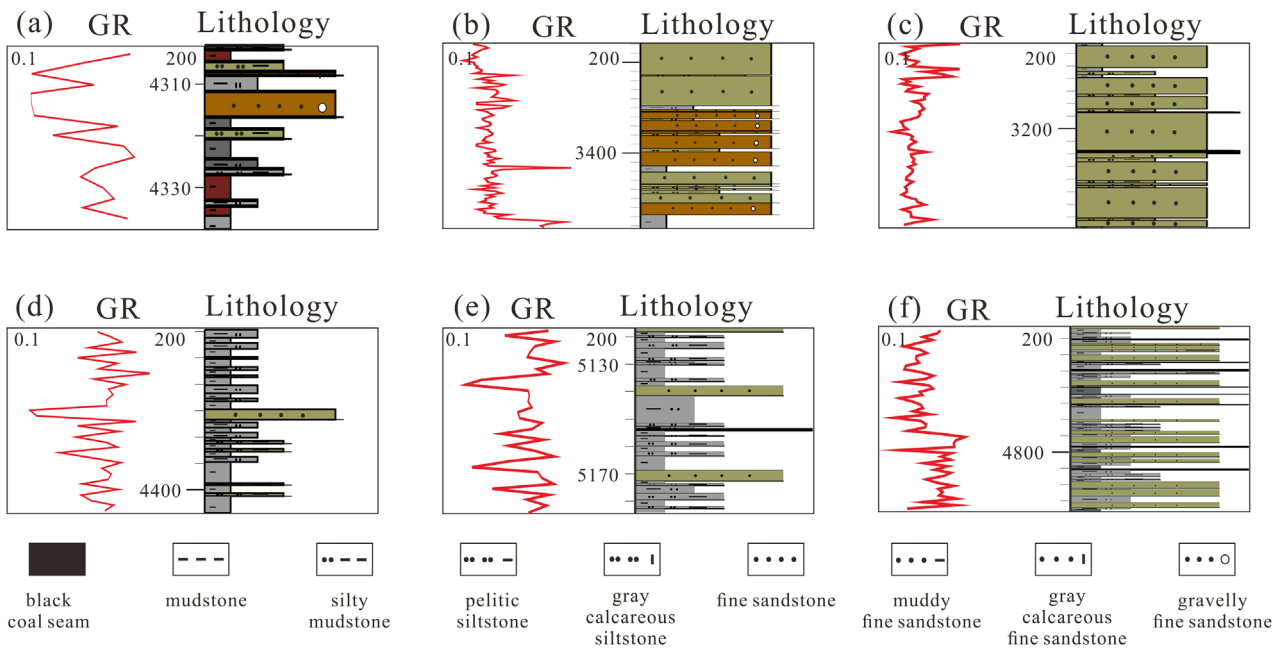

FIGURE 10
Representative well log patterns of different sedimentary facies types. **(a)** Natural levee; **(b)** Distributary channel; **(c)** Subaqueous distributary channel; **(d)** Interdistributary bay; **(e)** Mouth Bar; **(f)** Distal Bar.

depositional environment. Additionally, localized coal seams have been observed in some wells (Figure 9g), suggesting the occurrence of brief swamp conditions within the interdistributary bay areas.

5.3 Well log facies

Log facies refer to the interpretation of lithological types and depositional environ-ments based on characteristic patterns observed in well logging curves (Zhou, 2023; Kane et al., 2025). In this study, six types of sedimentary facies were identified: natural levee, distributary channel, subaqueous distributary channel, interdistributary bay, mouth bar, and distal bar. Natural levees are elongate ridges formed by fluvial deposition, typically consisting of interbedded thin layers of fine sandstone, siltstone, and mudstone. Reddish mudstone may also be present, indicating intermittent subaerial exposure along the riverbanks. On the gamma ray (GR) log, this facies generally displays a funnel-shaped curve (Figure 10a). Distributary channels are dominated by sandy deposits and exhibit a box-shaped GR curve, indicating relatively uniform, high-energy sedimentation (Figure 10b). Subaqueous distributary channels represent the seaward extension of distributary channels. Due to the damping effect of water, flow energy decreases, resulting in finer grain size and darker coloration than that of the fluvial distributary channel. The GR curve typically appears as bell-shaped or box-shaped (Figure 10c). Interdistributary bays are located in relatively low-lying areas between subaqueous distributary channels and are primarily composed of clay-rich deposits with minor silt content. The GR curve tends to be flat and of low amplitude (Figure 10d). Mouth bars form at the distal ends of subaqueous distributary channels, where flow energy rapidly decreases and clastic material is deposited under strong hydraulic resistance. These bars consist of silty mudstone and siltstone, arranged in a retrogradational sequence. On the GR log, they typically exhibit a moder-ate-amplitude funnel-shaped curve (Figure 10e). Distal bars, located further seaward of the mouth bars, are composed mainly of silt with minor clay and are identified by a moder-ate-amplitude finger-shaped GR curve (Figure 10f) (Ren et al., 2016).

5.4 Seismic facies

Seismic facies represent the integrated response of subsurface geological bodies and can be used to identify and predict sedimentary facies based on seismic reflection characteristics and various seismic attributes observed in seismic profiles (Liu et al., 2023b; Lin et al., 2022). The interpretation of sedimentary facies using seismic facies alone often carries a degree of uncertainty. Therefore, in this study, seismic facies interpretation is integrated with paleogeomorphic analysis, drilled well lithologic assemblages, and sedimentary environment characteristics. Additionally, existing research on the relationships between seismic facies and sedimentary facies in the Xihu Sag is referenced to support the interpretation of the study area. Based on the seismic profiles, the seismic facies of the Pinghu Formation can be broadly classified into four types, including medium-weak amplitude, shingled progradational reflection seismic facies, medium-weak amplitude, wavy to lens-shaped reflection seismic facies, strong amplitude, parallel to wavy reflection seismic facies and medium-strong amplitude, parallel-chaotic reflection seismic facies.

The medium-weak amplitude, shingled progradational reflection seismic facies is predominantly distributed within the

gentle uplift zones and the transitional zones between the slope and the basin. This facies is characterized by distinct, continuous, progradational reflection patterns that are systematically inclined, indicating the direction of sediment transport and accretion (Figures 11a, b). These progradational reflections suggest a sustained and orderly sediment supply, commonly associated with deltaic depositional processes. Based on its seismic characteristics and spatial distribution, this facies is interpreted to represent the sequential development of delta plain and delta front deposits, where sediments are progressively transported from the terrestrial source areas toward the basin.

The medium-weak amplitude, wavy to lens-shaped reflection seismic facies is mainly observed at the distal portions of the slope-basin transitional zones. These seismic reflections are typically discontinuous and exhibit irregular, lens-shaped geometries. This facies is commonly associated with the deposition of mouth bar subfacies, which predominantly develop in the distal delta front settings within the slope-basin transition. These mouth bars likely formed under the influence of fluctuating hydrodynamic conditions, where sediment supply periodically exceeded the capacity for transport, leading to the localized accumulation of sand bodies.

The strong amplitude, parallel to wavy reflection seismic facies is primarily distributed along the frontal margin of the central basin. This facies is characterized by laterally extensive, sheet-like sand bodies that display strong, continuous seismic reflections. The large-scale geometry of these sands, along with their seismic amplitude, suggests significant sand accumulation over broad areas. These sand bodies are interpreted as lenticular shelf sands that are spatially isolated from the delta front sands located in the western sector of the study area. Vertically, these sands often appear as stacked, multi-phase lenticular sand units, indicating episodic deposition likely controlled by fluctuating sea levels or tidal processes (Figure 11). This interval is considered to be associated with the widespread development of tidal-reworked bars, which are known to form under the influence of strong tidal currents in front of the delta system in the shallow marine shelf settings.

The medium-strong amplitude, chaotic reflection seismic facies is mainly developed in the deeper parts of the basin. This facies is characterized by disordered, irregular seismic reflections with poor continuity and low internal organization. Such chaotic seismic patterns are typically associated with complex depositional environments, often indicating the presence of shoreface to shallow marine settings where tidal and wave reworking processes dominate (Figure 11C). This interpretation is consistent with previous studies (Zhao, 2022), which suggest that tidal sand ridges were extensively developed within these deeper basin areas, driven by the interaction of strong tidal currents and variable sediment supply.

In addition to the medium-strong amplitude, chaotic reflection seismic facies, a medium-strong amplitude, parallel reflection seismic facies is also developed in close association with the chaotic facies. This parallel reflection facies is characterized by relatively continuous, uniform, and horizontally layered seismic reflections, which contrast with the disordered, low-continuity patterns typical of the chaotic facies. The presence of these parallel reflections suggests sedimentation under relatively stable hydrodynamic conditions, where the depositional energy was consistently low to moderate, allowing for the gradual and uniform accumulation of fine-grained sediments. The parallel reflection facies is interpreted to represent a more quiescent and stable depositional setting, likely corresponding to shallow marine shelf muddy deposits. Such environments are typically located further away from active deltaic or tidal sand ridge systems, where sediment input is dominated by suspended load rather than bedload transport. The fine-grained sediments, such as mudstones or silty mudstones, tend to settle from suspension under these calm conditions, leading to the development of well-bedded, laterally continuous layers. This facies may reflect periods of reduced sediment supply or diminished tidal influence, which promote the preservation of parallel stratification without significant reworking. The close spatial association between the chaotic and parallel facies suggests that these depositional environments may have alternated in response to fluctuations in sea level, tidal energy, or sediment supply.

5.5 Sedimentary facies distribution

Based on the paleogeomorphological reconstruction and extensive identification of core facies, log facies and seismic facies within the study area, a detailed characterization and planar prediction of sand body distribution within the Pinghu Formation has been carried out (Figure 12). This integrated approach provides a more robust geological framework for understanding the spatial variability of depositional systems in the region.

In the western part of the study area, various types of progradational reflection patterns are developed, indicating differences in sediment supply and depositional energy across the region. Specifically, the southern portion is dominated by medium-amplitude, shingled progradational reflections, the central part is characterized mainly by medium–weak amplitude, shingled progradational reflections, and the northern portion again exhibits medium-amplitude, shingled progradational reflections. These seismic reflection configurations are indicative of a basinward-prograding delta system, demonstrating the progressive advance of deltaic sediments into the deeper parts of the basin (Figure 12).

Adjacent to these shingled progradational seismic facies, particularly on the basin-ward side, strong-amplitude, parallel to wavy reflections are frequently observed. These seismic signatures are interpreted as mud-rich prodelta deposits, which typically accumulate in lower-energy settings located in front of the delta front.

In addition, within these strong-amplitude, parallel to wavy reflections representing prodelta mudstone units, there are also intermittently developed, banded seismic reflections characterized by medium–weak amplitude and wavy to parallel configurations (Figures 11C, 12). These features are interpreted as tidal sand ridge deposits that were formed under the influence of tidal currents, may indicate localized increases in energy within the prodelta setting. Unfortunately, we do not have wells that penetrate the tidal sand ridges, as the interpreted tidal sand ridge deposits are deeply buried. Currently, we also lack direct paleo-water depth evidence to support the interpretation of the tidal sand ridges. However, based on seismic interpretation, these deposits appear to have accumulated on a relatively gentle slope, which is more consistent with shallow marine shelf environments rather than deepwater settings. Future drilling activities in the basinal area may provide opportunities to

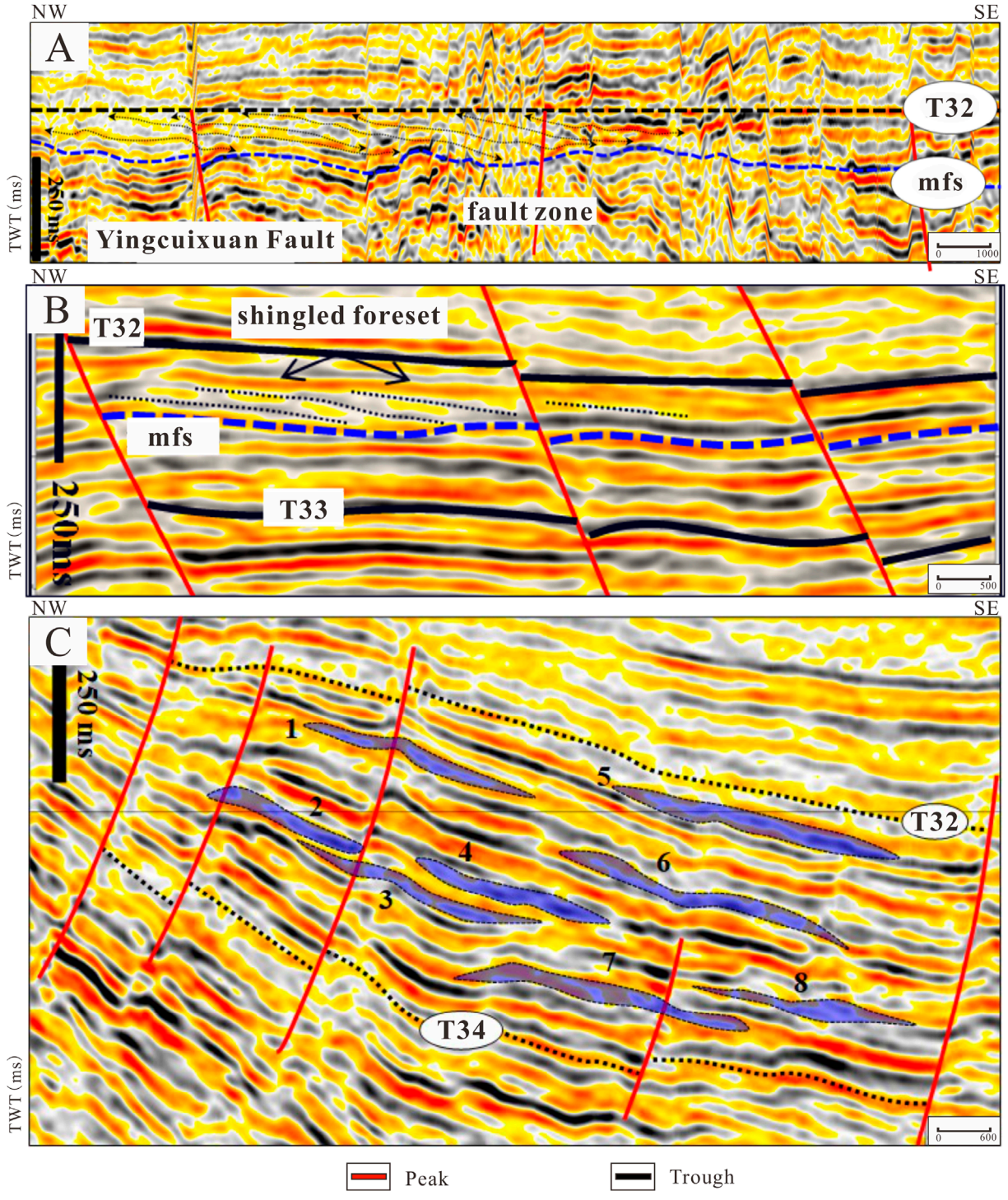

FIGURE 11
Representative seismic facies profiles of the study area. **(A)** and **(B)** seismic data indicates delta progradation from western slope to the basin; **(C)** Tidal ridge deposits in the basin area.

acquire tidal current simulation data or paleo-water depth evidence to further support this interpretation. Sedimentary facies analyses in the adjacent area to the south indicate there were tidal ridges deposits in the Xihu Sag during the Pinghu Formation (Wu et al., 2016), supporting our tidal ridge interpretaitons.

Further basinward, the seismic reflection patterns transition into medium-strong amplitude, parallel to chaotic reflections, which are typically associated with shallow marine environments. These zones represent the outermost extent of the deltaic influence and mark the transition into more open marine depositional conditions.

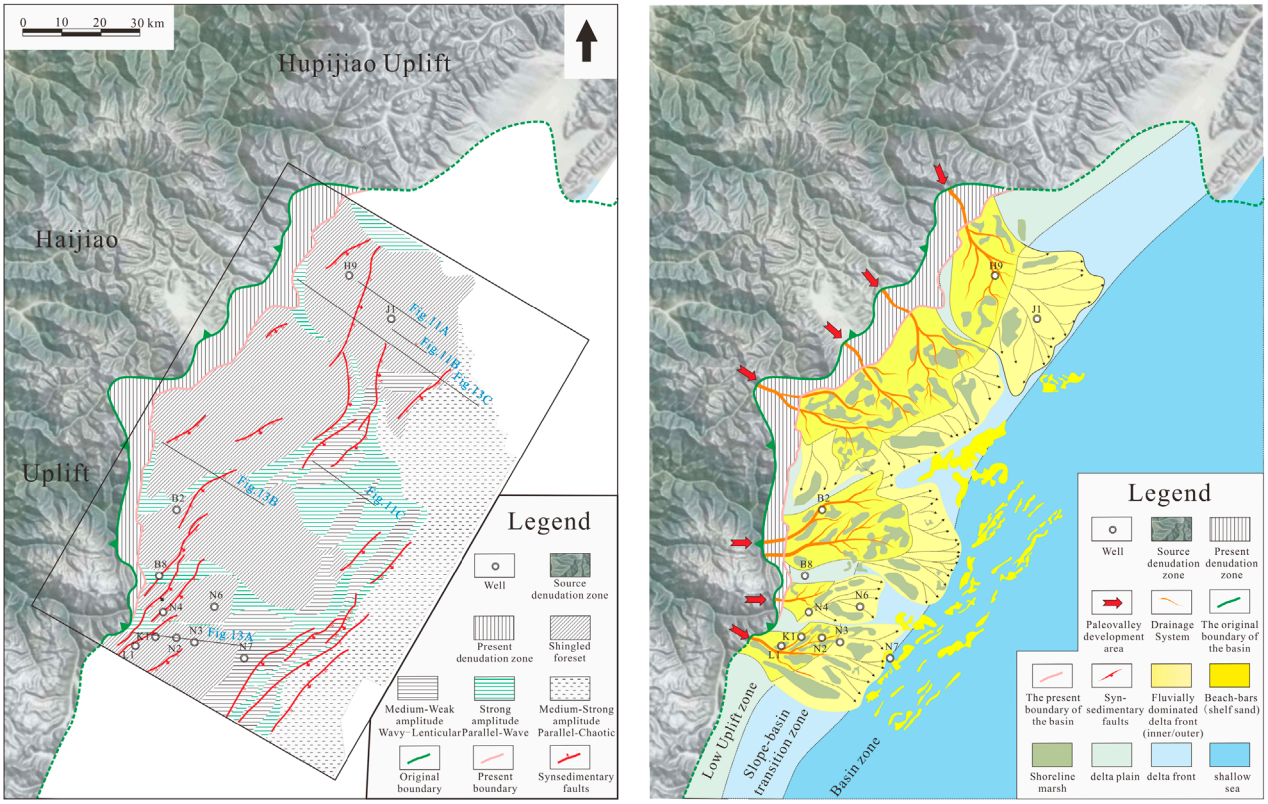

FIGURE 12
Plan view of seismic facies and sedimentary facies in the study area. Please note the development of the fault system influences the distribution of the sedimentary facies.

Integrated analysis of seismic profiles reveals that the sedimentary systems within the study area exhibit a distinct segmented pattern along the north-south direction. In the southern segment of the study area, the structural style is characterized by multi-fault, unidirectional transfer faults. Sediment transport is predominantly from west to east. Within this segment, a delta plain depositional system is well developed in the gentle uplift zones (low-amplitude paleo-highs). Further basinward, particularly at the slope-basin transition zone, delta front deposits are present, indicating a gradual shift from fluvial to more marine-influenced conditions. Additionally, tidal sand ridge deposits are observed overlying the submerged gentle uplifts, suggesting localized tidal reworking. In the central part of the basin, a shallow marine depositional system becomes dominant, reflecting a continued reduction in energy and increasing marine influence toward the basin center (Figure 13A).

In the central segment, the structural style is dominated by unidirectional single-fault systems, and fault development is relatively weak. Sediment transport also follows a west-to-east direction. The delta plain depositional system here is more extensively distributed, primarily developed over the low-amplitude uplift zones. The delta front system is primarily found in the slope-basin transition zone but also extends to the inner margin of the basin area. Within the central basin, shallow marine sediments dominate, with localized development of tidal sand ridges, indicating sporadic tidal influence in what is otherwise a relatively low-energy, offshore depositional setting (Figure 13B).

In the northern segment, multiple sets of unidirectional, source-aligned step-fault combinations are developed. This structural setting favors the development of a fluvially dominated delta system. Both the delta plain and delta front subfacies exhibit extended lateral continuity, reflecting relatively stable sediment supply and progradation potential (Figure 13C). A large-scale delta plain system is developed across the low-uplift zone, while the delta front depositional system is widely distributed in the slope-basin transition area. Notably, small-scale delta plain deposits are also observed in this transition zone, suggesting overlapping depositional processes. Within the basin area, delta front deposits are still present to some extent, accompanied by a prodelta muddy depositional system, indicating gradual energy dissipation and deepening basinward.

6 Influence of paleogeomorphology on sedimentary systems

The paleogeomorphological reconstruction suggests that the present-day erosional areas were capable of accumulating sediments during the depositional period of the Pinghu Formation. As shown in Figure 12, the boundary between the erosion and deposition zones can be restored over 10 km westward, indicating that delta plain deposits may have originally developed in these regions. This reconstruction provides valuable insights into

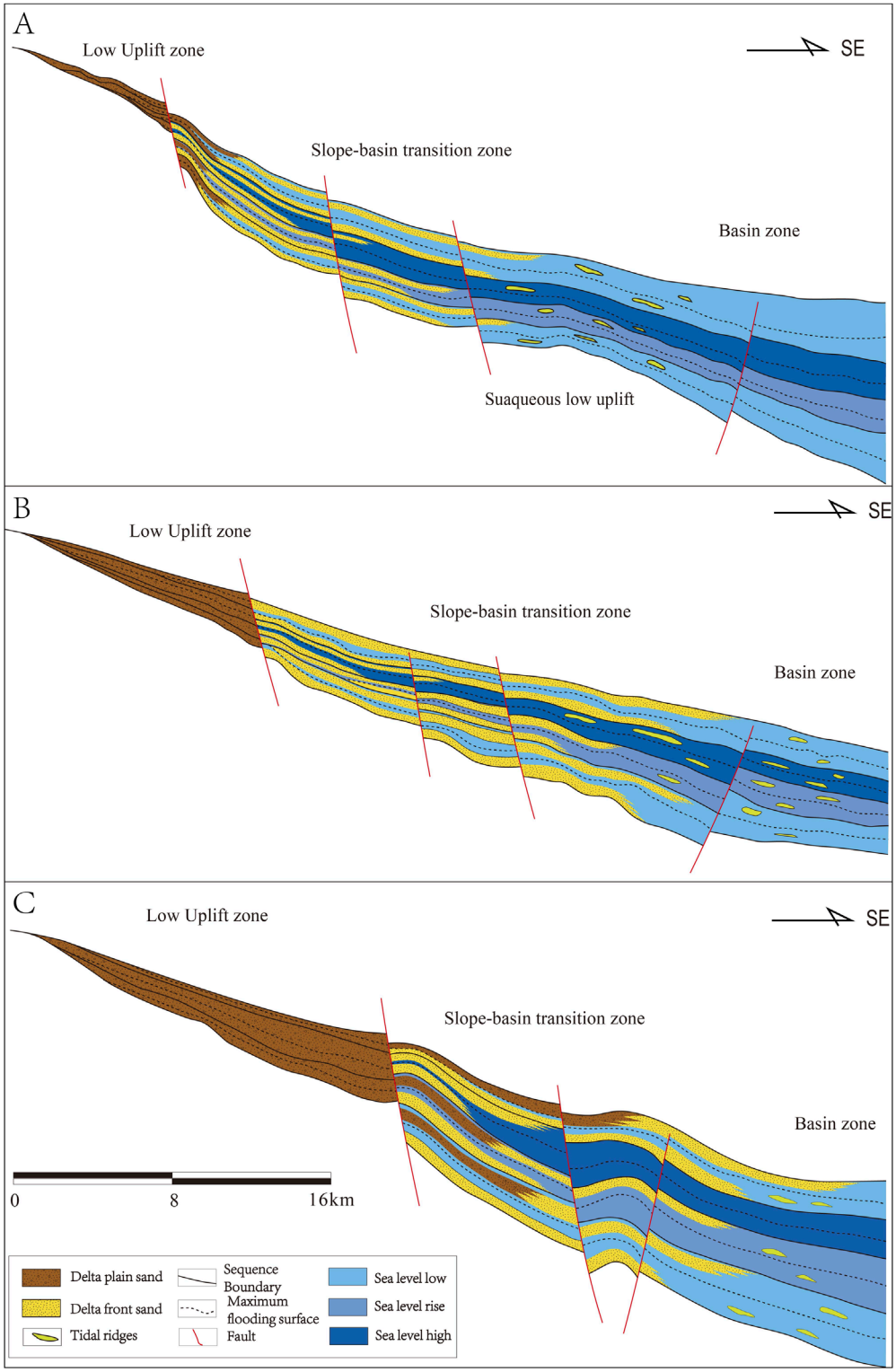

FIGURE 13
Sedimentary facies analysis of a representative seismic profile of the study area. **(A)** the southern part; **(B)** the central part; **(C)** the northern part. Please see location on Figure 12.

the source-to-sink system of the study area. For example, the reconstructed drainage area is significantly expanded, supporting the interpretation that large-scale delta systems were developed in this region. Furthermore, this paleogeomorphological framework may also have implications for the source-to-sink analysis of the overlying Huanggang Formation, which likely received recycled

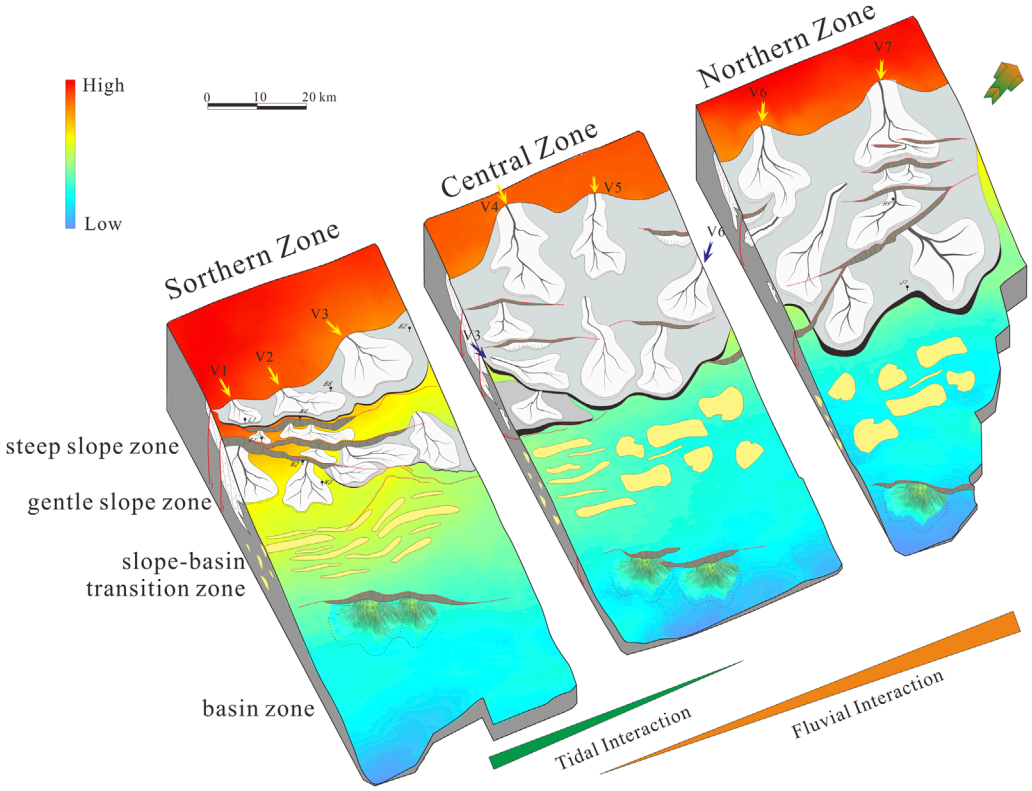

FIGURE 14
Paleogeomorphology and corresponding depositional facies of the study area.

sediments eroded from the previously deposited Pinghu Formation strata within the present-day denudation zones.

Through the reconstruction of paleogeomorphology and analysis of sedimentary systems in the study area, it is evident that different geomorphic configurations correspond to distinct combinations of sandbody-related depositional systems (Figure 14). This correlation highlights the fundamental control that paleogeomorphology exerts on sediment distribution, transport direction, and facies development.

From south to north, the study area displays clear spatial differentiation in geomorphologic and sedimentary characteristics. In the southern segment, the paleogeomorphology is relatively complex, with a high degree of structural deformation and a diversity of slope break types, including synthetic fault-related slope breaks, reverse fault-related slope breaks, and convergent fault-related slope breaks. Tectonic activity in this segment is strong, with the development of various fault combinations in both spatial and temporal dimensions. Sediment supply is abundant, and sediment transport directions are variable, reflecting the influence of multiple source areas. The dominant transport systems include oblique long-axis systems and short-axis systems oriented perpendicular to faults. These geomorphic and structural conditions favor the development of a composite depositional system consisting of delta plain in the gently uplift zone, delta front in the slope-basin transitional zone, and tidal sand ridge facies in the basin zone.

In the central segment, the overall geomorphology is characterized by a west-high, east-low topographic gradient. Sediment supply is stable and abundant, primarily sourced from the western Haijiao Uplift. The structural configuration is simpler than that of the southern segment, dominated by synthetic fault-related slope breaks. This region serves as a transitional zone, with low-relief terrain and poorly developed syndepositional faults. Sediment is primarily transported through paleo-valley systems, which are relatively broad and gentle. The low slope gradient favors the deposition of large-scale sand bodies with widespread but dispersed lateral distribution. The dominant depositional systems in this segment are delta plain and delta front, with minor development of shelf sand bodies at the outer edges of the delta front.

In the northern segment, the geomorphology is steeper, and the structural setting is dominated by NNE-trending, unidirectional normal faults. Slope break types are relatively simple and fewer in number, but large syndepositional faults are well developed. Sediment supply remains sufficient, although the source direction is more singular, primarily derived from the Haijiao Uplift in the west. Under these conditions, sand bodies supplied by the high-relief source area are transported downslope into the depression. Sediment is transported mainly through paleo-valley systems, and due to the steep slopes and fewer slope breaks, sand bodies tend to be large in scale and broadly distributed. The associated depositional systems include delta plain and delta front facies.

In summary, under the influence of varying paleogeomorphologic conditions, from south to north, the sediment transport distance increases, and the types and combinations of sedimentary systems vary accordingly. This demonstrates that paleogeomorphology

exerts a significant control over sandbody development and plays an important role in influencing the spatial distribution of sedimentary systems within the study area. From a west-to-east perspective, the study area shows a well-organized geomorphic and depositional framework. The western part is characterized by steep slope zones, which primarily serve as sediment source areas. To the east of these slope zones lies a gentle slope zone, where delta plain deposits are predominantly developed. Further east, the terrain transitions into a slope–basin mixed zone, where the delta front depositional system is well developed. In the central basin area, the dominant sedimentary environment shifts to a shoreface to shallow marine system, indicating progressive basinward deepening and declining depositional energy.

7 Conclusion

1. The paleogeomorphology of the Pinghu Formation exhibits clear north–south seg-mentation and east–west zoning, subdivided into southern, central, and northern segments, and into steep slope zone, gentle slope zone, slope-basin transition zone, and basin zones.
2. Paleogeomorphic features strongly influence sedimentary system types and sandbody distribution. The southern segment, with complex slope breaks and variable topography, hosts delta plain, delta front, and tidal sand ridge systems. The central segment, a transi-tional zone with gentle slopes, mainly develops delta plain and delta front systems, with minor shelf sands. The northern segment, characterized by steep slopes and simple fault patterns, also develops delta plain and delta front systems.
3. From west to east, the depositional systems transition from delta plain in gentle uplift zones, to delta front in slope–basin transition zones, and to shallow marine systems in the basin center, reflecting the strong control of paleogeomorphology on sedimentary system distribution.

These findings highlight the strong coupling between tectono-geomorphic evolution and sedimentary system development, and provide a valuable framework for future strati-graphic prediction and hydrocarbon exploration in the Xihu Sag.

Data availability statement

The raw data supporting the conclusions of this article will be made available by the authors, without undue reservation.

Author contributions

LQ: Writing – original draft. JX: Writing – review and editing. DX: Writing – review and editing. HL: Writing – review and editing. KC: Writing – review and editing.

Funding

The author(s) declare that no financial support was received for the research and/or publication of this article.

Acknowledgments

We thank the CNOOC Shanghai branch for allowing us to use and publish the data.

Conflict of interest

Authors LQ, DX, KC were employed by CNOOC Shanghai Branch.

The remaining authors declare that the research was conducted in the absence of any commercial or financial relationships that could be construed as a potential conflict of interest.

Generative AI statement

The author(s) declare that no Generative AI was used in the creation of this manuscript.

Publisher's note

References

Chen, S. H., Wang, J. W., Liu, S., Yan, S. M., Han, J. H., Fu, H., et al. (2025). Sedimentary characteristics of the middle member Pinghu Formation of Eocene in kongqueting area, xihu sag, east China Sea Shelf basin. *Lithol. Reserv.* 37 (02), 103–114. doi:10.12108/yxyqc.20250210

Cheng, Y. F., Dong, Y. L., Zhu, X. M., Yang, D. Q., Wu, W., Yang, K., et al. (2020). Cretaceous paleogeomorphology restoration and its controlling mechanism on sand-bodies in Chunguang exploration area, Junggar Basin. *J. Palaeogeogr. Ed.* 22 (06), 1127–1142. doi:10.7605/gdlxb.2020.06.076

Dai, L. M., Li, S. Z., Lou, D., Liu, X., Suo, Y. H., and Yu, S. (2014). Numerical modeling of late Miocene tectonic inversion in the xihu sag, east China Sea Shelf basin, China. *J. Asian Earth Sci.* 86, 25–37. doi:10.1016/j.jseaes.2013.09.033

Guo, K. W. (2014). *Main controlling factors of high-quality reservoir in Pinghu Group in the ramp region of Xihu depression*. Chengdu: Chengdu University of Technology. Master dissertation thesis.

Hou, G. F., Qu, J. H., Zhu, F., Xu, Y., Sun, J., Wang, L. B., et al. (2018). Controlling effect of paleogeomorphology on sedimentary system and sedimentary microfacies: a case study of Cretaceous Qingshuihe formation in the hinterland of Junggar basin. *J. China Univ. Min. and Technol.* 47 (05), 1038–1045. doi:10.13247/j.cnki.jcumt.000829

Hou, G. F., Wang, L. B., Song, B., Zeng, D. L., Jia, K. F., Dou, Y., et al. (2022). Analysis the controlling effect of paleogeomorphology on sedimentary systems: a case study of the Jurassic Sangonghe Formation in the central Junggar basin. *Acta Geol. Sin.* 96 (07), 2519–2531. doi:10.19762/j.cnki.dizhixuebao.2022102

Hou, G. W., Li, S., Qin, L. Z., Cai, K., Li, J. J., and He, M. (2019). Source-to-Sink system of Pinghu Formation in west slope belt of Xihu sag, East China Sea basin. *China Offshore Oil Gas* 31 (03), 29–39. doi:10.11935/j.issn.1673-1506.2019.03.004

Hu, M. Y., Shen, J., and Hu, D. (2013). Reservoir characteristics and its main controlling factors of the Pinghu Formation in Pinghu structural belt, Xihu Depression. *Oil and Gas Geol.* 34 (02), 185–191. doi:10.11743/ogg20130207

Huang, D. W., Duan, D. P., Liu, B. B., Liu, Y. H., and Huang, X. (2019). Reservoir characteristics and differential genesis of low permeability-tight sandstone gas reservoirs in Xihu sag. *China Offshore Oil Gas* 31 (03), 99–107. doi:10.11935/j.issn.1673-1506.2019.03.012

Huang, X., Lin, C. Y., Huang, D. W., Duan, D. P., Lin, J. L., He, X. K., et al. (2022). Diagenetic differential evolution of Huagang Formation sandstone reservoir in north-central part of central reversal structural belt in Xihu Sag. *Petroleum Geol. Recovery Effic.* 29 (02), 1–14. doi:10.13673/j.cnki.cn37-1359/te.2022.02.001

Jiang, D. H., Du, X. B., Li, K., and Zhou, F. (2022). Distribution of sedimentary system multi-controlled by palaeo-geomorphology, water system and break during the deposition of Pinghu Formation, Baochu slope belt,Xihu Sag, East China Sea Shelf Basin. *Petroleum Geol. and Exp.* 44 (05), 771–779. doi:10.11781/sysydz202205771

Jiang, Y. M., Zhou, Q. Y., Li, S., and Zhang, X. (2016). Reconsideration of Pinghu Formation coal-bearing rock series sedimentary environment in western slope of xihu depression. *Coal Geol. China* 28 (08), 18–25. doi:10.3969/j.issn.1674-1803.2016.08.04

Kane, O. I., Hu, M. Y., Cai, Q. S., Deng, Q. J., and Tong, Z. B. (2025). Sedimentary facies analysis, palaeogeography, and reservoir quality of the Middle-Upper Cambrian Xixiangchi Formation in southeast Sichuan Basin, southwest China. *J. Palaeogeogr.* 14 (01), 245–276. doi:10.1016/j.jop.2024.12.002

Li, L., Huang, X. S., Xiao, X. G., Zhang, T. L., and He, X. J. (2023). Sedimentary facies of Baoshi Formation in western slope zone of xihu sag. *Shanghai Land and Resour.* 44 (03), 23–27. doi:10.3969/j.issn.2095-1329.2023.03.004

Li, S., Yu, W. Z., Qin, L. Z., and Zhang, C. (2024). Sand-controlling model of source-slope break coupling in pinghu slope belt, xihu sag. *Mar. Geol. Front.* 40 (07), 36–44. doi:10.16028/j.1009-2722.2023.119

Li, S. L., Zhu, X. M., Li, H. Y., Liu, Q. H., and Shi, W. L. (2017). Quantitative characterization of elements and coupling mode in source-to-sink system: a case study of the Shahejie Formation between the Shaleitian uplift and Shanan sag, Bohai sea. *China Offshore Oil Gas* 29 (04), 39–50. doi:10.11935/j.issn.1673-1506.2017.04.005

Li, S. Q., and Li, C. J. (2003). Analysis on the petroleum resource distribution and exploration potential of the xihu depression, The East China sea. *Petroleum Geol. and Exp.* 25 (06), 721–728. doi:10.3969/j.issn.1001-6112.2003.06.015

Li, S. Q., Zeng, J. H., Liu, Y. Z., Li, M., and Jiao, P. P. (2023). Reservoir diagenesis and pore evolution of paleogene Pinghu Formation in kongqueting area of xihu sag,east China sea basin. *Lithol. Reserv.* 35 (05), 49–61. doi:10.12108/yxyqc.20230505

Li, W. H., Pang, J. G., Cao, H. X., Xiao, L., and Wang, R. G. (2009). Depositional system and paleogeographic evolution of the late triassic yanchang stage in ordos basin. *J. Northwest Univ. Sci. Ed.* 39 (03), 501–506. doi:10.16152/j.cnki.xdxbzr.2009.03.011

Li, X., Fu, L., Wei, P., Li, J. F., Xu, G., Cao, Q. Q., et al. (2025). Restoration of sedimentary paleogeography and its control on sedimentary system:A case study of the Triassic Baikouquan Formation in Shixi area of Junggar Basin. *Lithol. Reserv.* 37 (02), 38–48. doi:10.12108/yxyqc.20250204

Li, X. Q., Liu, J. S., Lu, Y. C., Jiang, Y. M., Du, X. B., and Chen, P. (2018). Prototype Basin chracterization of Huagang Formation of xihu depression, east China sea Shelf Basin. *Earth Sci.* 43 (02), 502–513. doi:10.3799/dqkx.2017.596

Li, Z. Y., Huang, Z. L., Ma, C. L., Zhang, W., Qu, T., Guo, X. B., et al. (2023). Reservoir quality control factors and pore evolution of Pinghu Formation in the western sub-sag of Xihu sag. *China Offshore Oil Gas* 35 (05), 47–60. doi:10.11935/j.issn.1673-1506.2023.05.005

Lin, C. S., Xia, Q. L., Shi, H. S., and Zhou, X. H. (2015). Geomorphological evolution, source to sink system and basin analysis. *Earth Sci. Front.* 22 (01), 9–20. doi:10.13745/j.esf.2015.01.002

Lin, H. M., Liu, H., Wang, D. X., Qiu, X. W., Ju, Y. T., Meng, J., et al. (2022). Basin-filling processes and hydrocarbon source rock prediction of low-exploration degree areas in rift lacustrine basins: a case from the Wenchang Formation in low-exploration degree areas, northern Zhu I Depression, Pearl River Mouth Basin, E China. *J. Palaeogeogr.* 11 (02), 286–313. doi:10.1016/j.jop.2022.03.002

Liu, C. X. (2010). Study on sedimentary facies for Pinghu Formation in pinghu oil and gas field in east China sea basin. *Offshore oil.* 30 (02), 9–13. doi:10.3969/j.issn.1008-2336.2010.02.009

Liu, F., He, W. J., Yang, L., Xu, W. X., and Ling, T. (2023). Seismic facies and sedimentary characteristics of shenhu Formation in the west of zhusan depression, the pearl river mouth basin. *Petroleum Geol. Eng.* 37 (05), 33–37. doi:10.3969/j.issn.1673-8217.2023.05.005

Liu, J. S., Zhang, G. D., and Liu, Y. (2023). Origin mechanism of abnormal high-pressure compartment in A sub-sag of Xihu sag and its controlling effect on reservoir formation. *China Offshore Oil Gas* 35 (03), 25–33. doi:10.11935/j.issn.1673-1506.2023.03.003

Liu, L., Chen, H. D., Wang, J., Zhong, Y. J., Du, X. F., Gan, X., et al. (2019). Geomorphological evolution and sediment dispersal processes in strike-slip and extensional composite basins: a case study in the Liaodong Bay Depression, Bohai Bay Basin, China. *Mar. Pet. Geol.* 110, 73–90. doi:10.1016/j.marpetgeo.2019.07.023

Liu, M. C., Wu, S. H., Yue, D. L., Xu, Z. H., Wan, X. L., Wu, H. L., et al. (2025). Palaeogeomorphological control on the depositional architecture of lacustrine gravity-flow deposits in a depression lacustrine basin: a case study of the Triassic Yanchang Formation, southern Ordos Basin, China. *J. Palaeogeogr.* 14 (02), 476–500. doi:10.1016/j.jop.2025.01.003

Liu, Y. R., Gao, S. L., Zhou, P., and Tang, X. J. (2020). Characteristics of transform faults in the xihu sag and their significance to hydrocarbon accumulation. *Mar. Geol. Front.* 36 (10), 42–49. doi:10.16028/j.1009-2722.2020.032

Lou, M., Cai, H., He, X. K., Liu, Y. H., Huang, X., Zhang, X. G., et al. (2023). Application of seismic sedimentology in characterization of fluvial-deltaic reservoirs in Xihu sag, East China Sea shelf basin. *Pet. Explor. Dev.* 50 (01), 138–151. doi:10.1016/s1876-3804(22)60375-6

Mioumnde, A. P., Zhang, L. Q., Yan, Y. M., Twinomujuni, L., Ran, H. W., Sedziafa, V., et al. (2025). Sedimentary facies architecture and terminal fan systems of the lower Palaeogene Shahejie Formation in Bonan sag, Bohai Bay Basin, China: implications for hydrocarbon exploration. *J. Palaeogeogr.* 14 (04), 100268–103836. doi:10.1016/j.jop.2025.100268

Mu, Z. H., Tang, Y., Cui, B. F., Xiao, Y. J., and Wang, G. L. (2002). Erosion thickness restoration in southwest tarim basin. *Acta Pet. Sin.* 23 (01), 40–44. doi:10.7623/syxb200201009

Ou, G. (2014). *Study of the paleostructure restoration of the early paleozoic, tarim basin*. Beijing: China University of Geosciences. Master dissertation thesis.

Qin, L. Z., Li, N., Xu, D. H., Sun, Z. H., and Wang, W. (2025). Fluvial to lacustrine alternating sedimentary characteristics of the Oligocene Huagang Formation in xihu sag, east China Sea Shelf basin. *Lithol. Reserv.* 37 (02), 178–188. doi:10.12108/yxyqc.20250216

Ren, S. P., Yao, G. Q., and Mao, W. J. (2016). Genetic types and superimposition patterns of subaqueous Distributary Channel thin sandbodies in delta front: a case study from the IV-VI reservoir groups of H3 in biqian 10 area of gucheng oilfield. *Acta Sedimentol. Sinca* 34 (03), 582–593. doi:10.14027/j.cnki.cjxb.2016.03.016

Shen, Y. L., Qin, Y., Cui, M., Xie, G. L., Guo, Y. H., Qu, Z. H., et al. (2021). Geochemical characteristics and sedimentary control of Pinghu Formation (Eocene) coal-bearing source rocks in xihu depression, east China sea basin. *Acta Geol. Sin. Ed.* 95 (01), 91–104. doi:10.1111/1755-6724.14624

Si, X. Q., Peng, B., Guo, H. J., Chen, X. G., Ji, D. S., Yi, J. F., et al. (2024). Sedimentary characteristic of retrogradational delta under paleo-geomor-phologic control and its petroleum geological significance: an example of the Qingshuihe Formation in central and eastern part of the southern margin in Junggar Basin. *Mar. Orig. Pet. Geol.* 29 (04), 401–412. doi:10.3969/j.issn.1672-9854.2024.04.006

Song, K., Lv, J. W., Du, J. L., and Wang, H. K. (2002). Source direction analysis and delta depositional systems of yanchang formation of the upper triassic in the central ordos basin. *J. Palaeogeogr. Ed.* (03), 59–66. doi:10.4236/gep.2023.118002

Wang, G. S., Zhou, Z. M., Xiao, C. H., Li, M. Z., Zhou, W. K., and Wang, L. (2002). Sedimentary characteristics of eogene pinghu formation and huagang formation in chunxiao zone of xihu lake depression. *Oil and Gas Geol.* 23 (03), 257–261+265. doi:10.11743/ogg20020312

Wang, H., Qin, L. Z., Li, S., Xu, D. H., and Xiao, X. G. (2024). Differential depositional characteristics under sequence stratigraphic framework and corresponding exploration strategies of the Pinghu Formation in Tiantai slope, xihu sag, east China sea basin. *J. Stratigr.* 48 (04), 419–429. doi:10.19839/j.cnki.dcxzz.2024.0030

Wang, T., He, C. R., Hu, H. J., Zhang, T. L., Tang, Y. J., Diao, H., et al. (2024). Crude oil source in the western slope zone of Xihu sag. *China Offshore Oil Gas* 36 (01), 37–48. doi:10.11935/j.issn.1673-1506.2024.01.004

Wang, W. Y., Cheng, H. G., Xu, S. J., Lin, Q., Huang, Y., Dong, X. Y., et al. (2023). Provenance indication and source characteristics of Huagang Formation in the central and western Xihu sag of the East China Sea basin. *China Offshore Oil Gas* 35 (02), 33–43. doi:10.11935/j.issn.1673-1506.2023.02.004

Wang, X., Li, F., Shen, J., Zhu, S. L., and Qi, P. (2022). Evolution of sedimentary system of Pinghu Formation in Hangzhou slope belt,Xihu sag. *Petroleum Geol. Recovery Effic.* 29 (04), 57–68. doi:10.13673/j.cnki.cn37-1359/te.202106044

Wei, G. C. (2014). *Erosion thickness restoration and palaeotectonics Analysis in TaBei and TaZhong area*. Beijing: China University of Geosciences. Master dissertation thesis.

Wei, H. F., Chen, J. F., Chen, X. D., Cao, B., Guo, W., and Zhang, J. H. (2013). The controlling factors and sedimentary environment for developing coastal coal-bearing source rock of Pinghu Formation in Xihu depression. *Geol. China* 40 (02), 487–497. doi:10.12029/gc20130213

Wu, L., Li, K., Zhou, F., Xie, C. Y., Tang, D. Q., and Zhang, Y. J. (2025). Characteristics and evolution of fault structures in Lengquanting area of Xihu Sag. *Mar. Geol. Front.* 41 (01), 31–43. doi:10.16028/j.1009-2722.2023.246

Xu, B. N., Liu, H., and Xu, J. (2025). Origin and evolution of large-scale sublacustrine fans in a lacustrine rift basin: a case study from the Liaozhong Depression (Bohai Bay Basin, E China). *J. Palaeogeogr.* 14 (02), 431–451. doi:10.1016/j.jop.2025.02.001

Xu, D. H., Qin, L. Z., Li, S., Cai, K., and Wang, Y. (2024). Sedimentary models and controlling factors of sand bodies in tidal flat environment of Pinghu Formation on Pingbei Slope of Xihu Sag. *China Offshore Oil Gas* 36 (05), 57–67. doi:10.11935/j.issn.1673-1506.2024.05.006

Yang, C. H., Gao, Z. H., Jiang, Y. M., and Gao, W. Z. (2013). Reunderstanding of clastic rock sedimentary facies of Eocene Pinghu Formation in pinghu slope of xihu sag. *J. Oil Gas Technol.* 35 (09), 11–14. doi:10.3969/j.issn.1000-9752.2013.09.003

Yang, Z., Wu, S. H., Duan, D. P., Xu, Z. H., Xiong, Q. C., and Zhang, Y. F. (2024). Architecture characteristics of distributary channels in shallow water delta plain of the Huagang Formation in Xihu sag, East China Sea. *J. Palaeogeogr. Ed.* 26 (03), 525–544. doi:10.7605/gdlxb.2024.03.049

Yu, K. D., Sun, L., Yan, S. M., Liu, S., Zuo, Y. W., and Hao, W. H. (2024). Analysis of the "Source-ditch-sink" and sedimentary system of Baoshi Formation in the K gas field of xihu sag. *Offshore oil.* 44 (02), 15–21. doi:10.3969/j.issn.1008-2336.2024.02.015

Zhang, J. Y., Pas, D., Krijgsman, W., Wei, W., Du, X. B., Zhang, C., et al. (2020). Astronomical forcing of the paleogene coal-bearing hydrocarbon source rocks of the East China Sea Shelf basin. *Sediment. Geol.* 406, 105715. doi:10.1016/j.sedgeo.2020.105715

Zhang, L., He, X. K., Duan, D. P., Cheng, J. Y., Chen, C., and Wang, W. J. (2022). Potential of subtle hydrocarbon reservoirs in paleo-valleys in the Pingxi area of Xihu Sag. *Mar. Geol. Front.* 38 (01), 41–50. doi:10.16028/j.1009-2722.2021.052

Zhang, S. L., Zhang, J. P., Tang, X. J., and Zhang, T. (2014). Geometry characteristic of the fault system in xihu sag in east China sea and its formation mechanism. *Mar. Geol. and Quat. Geol.* 34 (01), 87–94. doi:10.3724/SP.J.1140.2014.01087

Zhang, Y. Z., Hu, S. Q., Liu, J. S., Chen, Z. Y., Jiang, Y. M., Zhou, W., et al. (2022). Gas accumulation conditions and mode in X sag of East China Sea Basin. *China Offshore Oil Gas* 34 (01), 27–35. doi:10.11935/j.issn.1673-1506.2022.01.004

Zhao, J. X., Chen, H. D., and Shi, Z. Q. (2001). The way and implications of rebuilding palaeogeomorphology–Taking the research of palaeogeomorphology of the Ordos Basin before Jurassic deposition as example. *J. Chengdu Univ. Technol. (Sci. & Technol.)* 28 (3), 260–266.

Zhao, L. N., Chen, L. W., Zhang, Y. G., Cheng, X. M., and Sha, X. G. (2008). Sedimentary characteristics of Pinghu Formation in pinghu structural belt of xihu depression, east China sea. *World Geol.* 27 (01), 42–47. doi:10.3969/j.issn.1004-5589.2008.01.008

Zhao, Q. (2022). *Tidal and river joint-dominated sedimentary system analysis of the Pinghu Formation in the west slope belt of Xihu depression, east China Sea Shelf basin*. Wuhan: China University of Geosciences. Doctoral dissertation thesis. doi:10.27492/d.cnki.gzdzu.2022.000177

Zhao, Z. G., Wang, P., Qi, P., and Guo, R. (2016). Regional background and tectonic evolution of east China sea basin. *Earth Sci.* 41 (03), 546–554. doi:10.3799/dqkx.2016.045

Zhou, S. Y. (2023). *Study on delta sedimentary microfacies recognition method based on deep learning*. Beijing: China University of Petroleum. Master dissertation thesis. doi:10.27643/d.cnki.gsybu.2023.001240